applied sciences

MDPI

Article

A Comparison of Different District Integration for a Distributed Generation System for Heating and Cooling in an Urban Area

Melchiorre Casisi [1,*], Dario Buoro [1], Piero Pinamonti [1] and Mauro Reini [2]

[1] Polytechnic Department of Engineering and Architecture, University of Udine, 33100 Udine, Italy
[2] Department of Engineering and Architecture, University of Trieste, 34100 Trieste, Italy
* Correspondence: melchiorre.casisi@uniud.it; Tel.: +39-338-9946-864

Received: 16 July 2019; Accepted: 21 August 2019; Published: 27 August 2019

Abstract: The paper proposes a comparison of different district integration options for a distributed generation system for heating and cooling in an urban area. The system considered includes several production units located close to the users, a central unit and the district heating and cooling network which can connect all the users to each other and to a central unit, where a cogeneration system and a solar plant can be placed. Thus, each user can be regarded as isolated from the others, satisfying its energy needs by means of an autonomous production unit. Alternatively, it can be connected to the others through the district heating and cooling network. When a district heating and cooling network is included in the design option the synthesis-design and operation problems cannot be solved separately, because the energy to be produced by each production site is not known in advance, as the flows through the district heating and cooling network are not defined. This paper uses a mixed integer linear programming (MILP) methodology for the multi-objective optimization of the distributed generation energy system, considering the total annual cost for owning, operating and maintaining the whole system as the economic objective function, while the total annual CO_2 emissions as the environmental objective function. The energy system is optimized for different district integration option, in order to understand how they affect the optimal solutions compared with both the environmental and economic objects.

Keywords: district heating and cooling; multi-objective optimization; distributed cogeneration; optimal operation

1. Introduction

The reduction of pollutant emissions is one of the current main targets fixed by international authorities. A lower energy need in the residential and tertiary sectors can help to achieve this goal, as it represents one of the dominant energy consuming sectors in industrialized societies. However, the adoption of a defined energy system still depends on technical and financial evaluations, while environmental aspects are not generally regarded as design goals.

A review of the open literature on these topics shows that the current research works can be grouped into three major groups:

- research focusing on the optimization of the operation of energy systems, ranging from the optimization of a single component, to the operation of the overall DG system;
- research dealing with the optimization of the system synthesis; and
- research focusing on synthesis, design and operation optimization.

Each group can be further subdivided, considering single and multi-objective optimization targets.

Over the last decade an increasing number of papers dealing with energy system optimization have been produced [1]. One of the first optimization models was developed by Henning in 1992 [2], and consists of a linear programming model to minimize the operating cost of an energy supply system for local Swedish utilities. In 1997 he presented a linear programming model called MODEST [3] for the minimization of capital and operation costs of energy supply and demand side management. Curti et al. [4] proposed an optimization model for aiding the design of a mixed energy production system, including heat pump based district heating, conventional boilers and decentralized heat pump. Yokoyama et al. [5] in 2002 proposed a method for optimal structural design, to determine the structures of energy supply systems in consideration of their multi-period operation. Karlsson [6] has recently presented the MIND method, a decision support for optimization of industrial energy systems.

For a general overview of models, methods and applications of multi-utility energy systems, the authors refer readers to extended reviews presented recently [1,7–10]. Among a large quantity of research presented in this field, some common points can be outlined:

- almost all models rely on linear programming or mixed integer linear programming (MILP). However, some approaches based on meta-heuristics (simulated annealing, genetic algorithms, etc.) have been proposed, but they present some difficulties concerning the determination of search parameters and the judgment about optimality [11–13].
- the research normally focus only on specific targets: operation or synthesis optimization, economic and/or environmental optimization, unit or district heating network (DHN) optimization, etc.

To deal with optimization of DG energy systems, including DHCN and thermal storage, and focusing on different objectives (economic rather than environmental), it is necessary to consider all aspects at the same time, and not in successive steps. This is because the operation optimization strongly affects the optimal synthesis of the system and, in addition, the economic optimum does not correspond to the environmental one.

Some recent papers seem to go in this direction, performing a single objective optimization, generally economic: Chinese proposed a MILP model for the optimization of a DHCN in a DG context [14], Soderman and Petterson [15] presented a structural and operational optimization of a DG energy system. Pavicevic et al. [16] performed the optimization of sizing and operation of a DH system, focusing on the technological options for the TS. Pérez-Mora et al. [17] optimized DHC systems, focusing on the alternative between absorption and compression chillers. Ameri and Besharati [18] defined a model for determining the optimal capacity and operation of seven combined cooling, heating and power (CCHP) systems in the heating and cooling network of a residential complex located east of Theran.

Finally, Ren et al. [19] proposed a multi-objective optimization model to analyse the optimal operating strategy of a distributed energy system, while combining the minimization of energy costs with the minimization of environmental impact, which is assessed in terms of CO_2 emissions. Carvalho [20] presented a model for the synthesis and operation optimization of residential units, considering environmental and economic aspects.

In this paper, the optimization MILP model is applied to a real case study, made up of nine tertiary sector users located in a small town city centre situated in the northeast of Italy. A preliminary energy audit allowed the determination of the users' energy needs, so that the latter is regarded as the input of the optimization procedure.

This paper proposes a comparison of different district integration option for a distributed generation (DG) system for heating and cooling in an urban area. The distributed generation energy system considered in the paper includes several production units located close to the users, a central unit and the district heating and cooling network (DHCN) which can connect all the users to each other and to a central unit, where a cogeneration system and a solar plant can be placed. Thus, each user can be regarded as isolated from the others, satisfying its energy needs by means of an autonomous production unit. Alternatively, it can be connected to the others through the DHCN. In this case, it

can produce its needs and feed other users, or can only receive energy from the network without any "internal" production, or both. When a DHCN is included in the design option the synthesis-design and operation problems cannot be solved separately, because the energy to be produced by each production site is not known in advance, as the flows through the DHCN are not defined. Thus, a model for the simultaneous definition of the optimal synthesis, design and operation has been developed. The model uses a MILP methodology for the multi-objective optimization of the DG energy system, considering the total annual cost for owning, operating and maintaining the whole system as the economic objective function, while the total annual CO_2 emissions as the environmental objective function.

The synthesis, design and operation of the energy system have been simultaneously optimized for different district integration options, in order to understand how they affect the optimal solutions compared with both the environmental and financial objectives.

2. MILP Model

The mathematical problem of optimizing the synthesis, design and operation of a DG energy system has to be generally regarded as a variational calculus problem because several decision variables related to the components are time dependent. However, a realistic description of the system may be represented by a MILP formulation by properly discretizing all dynamic variables in quasi-stationary variables and approximating all non-linear relations in a set of linear functions [5,21–24]. To solve the issue of synthesizing the configuration of the energy system, a reducible structure (known also as a superstructure) which embeds several possible configurations and interconnections is defined.

The superstructure proposed in this research is shown in Figure 1. The superstructure can be divided into two different parts: the superstructure related to each *site*; and the superstructure related to the *central unit*. The green, red and blue lines represent the physical distribution of electric, thermal and cooling energy, respectively, while the orange arrows represent the fuel inputs. Following each distribution line inside the site *k*, the electricity can be produced by internal combustion engines (ICE), by micro gas turbines (MGT) and by photovoltaic panels (PV), can be bought from or sold to the electricity grid, used by compression chillers (CC) and by the heat pumps (HP), while the rest is sent to the user *k*. The thermal energy can be produced by ICEs, by MGTs, by solar thermal (ST) panels, by boilers (BOI) and by HPs, can be stored in the thermal storage (TS), can be used by absorption chillers (ABS), can be send to the user *k* or to the DHN. The cooling energy can be produced by CCs, by ABSs and by HPs, can be stored in the cooling storage (CS), can be sent to the user *k* or to the district cooling network (DCN). The central unit can produce electricity by the centralized ICE, can produce thermal energy by the same ICE, by the central BOI and by the solar thermal field (ST field). The thermal energy produced in the central unit can be sent directly to the DHN and then to the users, or can be stored in a centralized TS and used later. The electricity produced in the central unit by the centralized ICE can only be sold to the electricity grid [22].

The superstructure shown in Figure 1 has been created specifically for the problem involved in the study, but it is general and can be integrated with other components. It can be modified with different connections of the components or it can be reduced by eliminating some components considered superfluous. The number of users is not defined a priori; however, it is limited by the computational effort which is quadratic whit the overall number of decision variables.

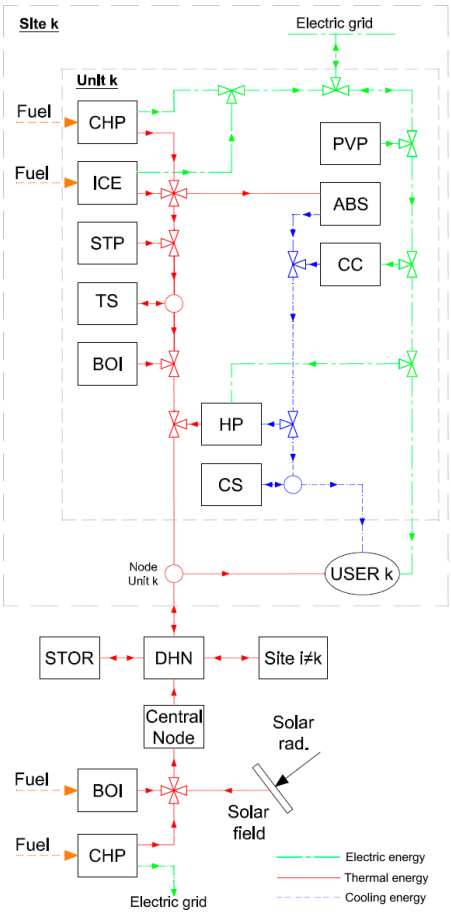

Figure 1. Superstructure of the distributed generation solution (integrated with central solar system).

2.1. Decision Variables and Constraints

The optimization variables to be considered in order to determine the optimal configuration and operation of the DG energy system can be divided into two main groups:

- binary variables: they represent the existence/absence of each component and the operation status (on/off) of each component in each time interval. There are other additional binary variables which do not represent any physical quantity, added to linearize some relations; and
- continuous variables: they represent the size of components, the size of pipelines, the load of components in each time interval, the energy content of the storages and the connection flows.

The performance characteristics of equipment and energy balance relationships are the fundamental constraints of the optimization problem. Other constraints, such as relationships between maximum contract demands and consumption of energy purchased and operational restrictions, have also to be considered. In the MILP model, equality constraints express fix relations and balances, while inequality constraints, express limits and feasibility conditions. The constraints can be generally grouped into four categories which describe:

- components;
- district heating and cooling network;
- thermal storage; and
- energy balances.

2.2. Components

All cogenerators, heat pumps and absorption chillers included in the superstructure are of fixed size, while boilers, compression chillers, solar and photovoltaic panels are of variable size. Up to j components of the same fixed size can be adopted in parallel by the same user. The components of the central unit are all of variable size. The following constraints (Equations (1)–(5)) describe the linear model of ICE which can be installed in each production site.

The first set of constraints ensures that a consistent set of binary variables ($\boldsymbol{X_{ice}}$, $\boldsymbol{O_{ice}}$) is taken into account in each time interval and throughout the year: the component j can be installed only if the component $j-1$ has been already adopted (Equation (1)), and the component j can never be in operation if it has not been adopted (Equation (2)):

$$\boldsymbol{X_{ice}}(j,u) \leq \boldsymbol{X_{ice}}(j-1,u) \tag{1}$$

$$\boldsymbol{O}_{ice}(m,d,h,j,u) \leq \boldsymbol{X}_{ice}(j,u) \tag{2}$$

The second group describes the partial load performance of energy conversion devices by means of linear relations:

$$H_{ice}(m,d,h,j,u) = Kh_{ice}(m,d,h,1)\cdot\boldsymbol{E_{ice}}(m,d,h,j,u) + Kh_{ice}(m,d,h,2)\cdot\boldsymbol{O_{ice}}(m,d,h,j,u) \tag{3}$$

$$F_{ice}(m,d,h,j,u) = Kf_{ice}(m,d,h,1)\cdot\boldsymbol{E_{ice}}(m,d,h,j,u) + Kf_{ice}(m,d,h,2)\cdot\boldsymbol{O_{ice}}(m,d,h,j,u) \tag{4}$$

$$E_{ice,lim}(m,d,h,u,1)\cdot\boldsymbol{O_{ice}}(m,d,h,j,u) \leq \boldsymbol{E_{ice}}(m,d,h,j,u) \leq E_{ice,lim}(m,d,h,u,2)\cdot\boldsymbol{O_{ice}}(m,d,h,j,u) \tag{5}$$

The coefficients Kh_{ice} and Kf_{ice} can be obtained through a linear regression of the load curves. The constraints which describe the MGT can be easily inferred by changing in each variable or coefficient the subscript "*ice*" with the subscript "*mgt*". A variable size ICE can be installed in the central unit. The constraints which describe this component (Equations (6)–(12)) are different from the previous constraints, because both size and load are decision variables. Therefore, it is necessary to introduce additional constraints and decision variables in order to maintain the linearity of the problem.

The first set of constraints limits the size of the ICE which can be adopted and put in relation the operation with the existence of the component:

$$S_{ice,lim,c}(1)\cdot\boldsymbol{X_{ice,c}} \leq \boldsymbol{S_{ice,c}} \leq S_{ice,lim,c}(2)\cdot\boldsymbol{X_{ice,c}} \tag{6}$$

$$\boldsymbol{O}_{ice,c}(m,d,h) \leq \boldsymbol{X}_{ice,c} \tag{7}$$

The second set of constraints expresses the relations among the main product ($\boldsymbol{E_{ice,c}}$), the sub-product ($H_{ice,c}$) and the fuel flows ($F_{ice,c}$):

$$H_{ice,c}(m,d,h) = Kh_{ice,c}(m,d,h,1)\cdot\boldsymbol{E_{ice,c}}(m,d,h) + Kh_{ice,c}(m,d,h,2)\cdot\boldsymbol{O_{ice,c}}(m,d,h) + Kh_{ice,c}(m,d,h,3)\cdot\boldsymbol{\xi}_{ice,c}(m,d,h) \tag{8}$$

$$F_{ice,c}(m,d,h) = Kf_{ice,c}(m,d,h,1)\cdot\boldsymbol{E_{ice,c}}(m,d,h) + Kf_{ice,c}(m,d,h,2)\cdot\boldsymbol{O_{ice,c}}(m,d,h) + Kf_{ice,c}(m,d,h,3)\cdot\boldsymbol{\xi}_{ice,c}(m,d,h) \tag{9}$$

The last set of equations is required to constrain the additional variables $\boldsymbol{\xi}_{ice,c}(m,d,h)$, which allow us to introduce a linear relation with two independent variables—size $\boldsymbol{S_{ice,c}}$ and load $\boldsymbol{E_{ice,c}}(m, d, h)$—avoiding inconsistent results when the engine is off:

$$\boldsymbol{S_{ice,c}} + S_{ice,lim,c}(2)\cdot(\boldsymbol{O_{ice,c}}(m,d,h) - 1) \leq \boldsymbol{\xi}_{ice,c}(m,d,h) \leq \boldsymbol{S_{ice,c}} \tag{10}$$

$$S_{ice,lim,c}(1)\cdot\boldsymbol{O_{ice,c}}(m,d,h) \leq \boldsymbol{\xi}_{ice,c}(m,d,h) \leq S_{ice,lim,c}(2)\cdot\boldsymbol{O_{ice,c}}(m,d,h) \tag{11}$$

$$\boldsymbol{E}_{ice,c}(m,d,h) \leq \boldsymbol{S}_{ice,c} \tag{12}$$

The boiler which can be installed in the central unit is described by the following equations (Equations (13)–(16)), where a minimum load limit ($H_{boi,lim,c}$ = 0.1) has been taken into account and auxiliary variables $\boldsymbol{\psi_{boi,c}}(m, d, h)$ play a role analogous to variables $\boldsymbol{\xi}_{ice,c}(m, d, h)$, previously introduced for the ICE:

$$F_{boi,c}(m,d,h) = \boldsymbol{H_{boi,c}}(m,d,h)/\eta_{boi,c}(m,d,h) \quad (13)$$

$$H_{boi,lim,c} \cdot \boldsymbol{\psi_{boi,c}}(m,d,h) \leq \boldsymbol{H_{boi,c}}(m,d,h) \leq \boldsymbol{\psi_{boi,c}}(m,d,h) \quad (14)$$

$$\boldsymbol{S_{boi,c}} + S_{boi,lim,c}(2)\cdot(\boldsymbol{O_{boi,c}}(m,d,h) - 1) \leq \boldsymbol{\psi_{boi,c}}(m,d,h) \leq \boldsymbol{S_{boi,c}} \quad (15)$$

$$S_{boi,lim,c}(1)\cdot\boldsymbol{X_{boi,c}} \leq \boldsymbol{S_{boi,c}} \leq S_{boi,lim,c}(2)\cdot\boldsymbol{X_{boi,c}} \quad (16)$$

The boilers and the compression chiller installed in the production sites have been modelled by means of the efficiency and the COP alone, without a minimum load limit.

Absorption chillers are modelled like local ICE and GT, as components of fixed size which can be installed as multiple units operating in parallel. Each ABS operation is allowed only if the heat produced by ICE and MGT, in the same site, is greater than the heat required by the former and the ABS existence is constrained by the existence of ICE and MGT, as expressed by Equations (17) and (18):

$$\boldsymbol{C_{abs}}(m,d,h,j,u) \leq H_{ice}(m,d,h,j,u) + H_{mgt}(m,d,h,j,u) \quad (17)$$

$$\boldsymbol{X_{abs}}(j,u) \leq \boldsymbol{X_{ice}}(j,u) + \boldsymbol{X_{mgt}}(j,u) \quad (18)$$

The heat pump is modelled as a black box that can produce either heat—$\boldsymbol{O_{hp,h}}(m, d, h, j, u) = 1$—or cold—$\boldsymbol{O_{hp,c}}(m,d,h,j,u) = 1$, but not simultaneously:

$$X_{hp}(j,u) \leq X_{hp}(j-1,u) \quad (19)$$

$$\boldsymbol{O_{hp,h}}(m,d,h,j,u) \leq \boldsymbol{X_{hp}}(j,u) \quad (20)$$

$$\boldsymbol{O_{hp,c}}(m,d,h,j,u) \leq \boldsymbol{X_{hp}}(j,u) \quad (21)$$

$$\boldsymbol{O_{hp,h}}(m,d,h,ju) + \boldsymbol{O_{hp,c}}(m,d,h,j,u) \leq 1 \quad (22)$$

$$H_{hp}(m,d,h,j,u) = K_{hp}(m,d,h,u,1)\cdot\boldsymbol{E_{hp,h}}(m,d,h,j,u) + K_{hp}(m,d,h,u,2)\cdot\boldsymbol{O_{hp,h}}(m,d,h,j,u) \quad (23)$$

$$C_{hp}(m,d,h,j,u) = K_{hp}(m,d,h,u,3)\cdot\boldsymbol{E_{hp,c}}(m,d,h,j,u) + K_{hp}(m,d,h,u,4)\cdot\boldsymbol{O_{hp,c}}(m,d,h,j,u) \quad (24)$$

$$S_{hp,lim}(m,d,h,u,1)\cdot\boldsymbol{O_{hp,h}}(m,d,h,j,u) \leq \boldsymbol{E_{hp,h}}(m,d,h,j,u) \leq S_{hp,lim}(m,d,h,u,2)\cdot\boldsymbol{O_{hp,h}}(m,d,h,j,u) \quad (25)$$

$$S_{hp,lim}(m,d,h,u,1)\cdot\boldsymbol{O_{hp,c}}(m,d,h,j,u) \leq \boldsymbol{E_{hp,c}}(m,d,h,j,u) \leq S_{hp,lim}(m,d,h,u,2)\cdot\boldsymbol{O_{hp,c}}(m,d,h,j,u) \quad (26)$$

$$E_{hp}(m,d,h,j,u) = \boldsymbol{E_{hp,h}}(m,d,h,c,u) + \boldsymbol{E_{hp,c}}(m,d,h,j,u) \quad (27)$$

Equations (23) and (24) refer to the characteristic curve of the heat pump in the heating and cooling mode, respectively. The solar thermal collectors and the photovoltaic panels are modelled considering their production proportional to the size of the plants. The unitary production—$K_{stp}(m, d, h, u)$ and $K_{pv}(m, d, h, u)$—is evaluated a priori considering inclination, orientation angle of installation and hourly solar radiation of the site of the plant.

2.3. District Heating and Cooling Network

The modelling of the DHCN is important for the optimization of the DG energy system, because it strongly affects the optimal solution [25–27]. The aim of the DG energy system optimization, is to define the lay-out of the DHCN and the dimension of each single pipeline, taking into account the operation of the whole system. The heat which can be transferred by a DHCN pipeline can be expressed by:

$$\dot{Q}_p = A_p\cdot v_p\cdot\rho_p\cdot c_p\cdot\Delta t \quad (28)$$

Assuming that the velocity v_p is fixed, the transferred heat $\dot{Q}_p$ reported in Equation (28) depends on two variables, which are the cross section of the pipeline A_p and the temperature difference between inlet and outlet pipelines Δt [28]. Assuming a fixed temperature of the network and a fixed temperature difference between the inlet and outlet, the modelling introduces a constant ratio between the size of the pipeline and the maximum flow which can be transferred, and considers the size and the layout of the network as decision variables, constrained by the pipeline super-structure and the flow rate limits of each pipe. The Δt adopted normally ranges between 15–25 °C depending on the application, while the medium velocity v_p ranges between 1.5–2.5 m/s. The thermal losses are considered proportional to the length of each pipeline through the coefficient δ_t:

$$p_t(u,v) = \delta_t \cdot l_p(u,v) \tag{29}$$

Equations (30)–(32) describe the existence conditions of thermal pipelines, the energy flow through each pipeline during operation and the maximum flow characterizing the size of each pipeline:

$$\boldsymbol{X_{tp}}(u,v) + \boldsymbol{X_{tp}}(v,u) \leq 1 \tag{30}$$

$$H_{net,lim}(1)\cdot\boldsymbol{X_{tp}}(u,v) \leq \boldsymbol{S_{H,net}}(u,v) \leq H_{net,lim}(2)\cdot\boldsymbol{X_{tp}}(u,v) \tag{31}$$

$$\boldsymbol{H_{net}}(m,d,h,u,v) \leq \boldsymbol{S_{H,net}}(u,v) \tag{32}$$

The same modelling can be obtained for the district cooling network, by changing properly the subscripts.

2.4. Thermal Storage

A long-term thermal storage might be able to extend the operation time of the combined heat and power (CHP) unit. In fact, during summer time, for instance, the heat demand can be so low that the CHP plant must be shut down and a boiler, which is often expensive in terms of operational cost, must be brought into operation. By using a thermal storage, power generation can be increased and the use of fossil fuels can be reduced [29]. The problem of intermittent energy sources is especially severe for solar energy, because thermal energy is usually needed most when solar availability is lowest, namely, in winter. Small TS can cover periods of inadequate sunshine, while large TS, operating over long period, can partially cover the lower winter solar thermal production [30]. In any case, the design of the integrated system is very difficult and normally several rules of thumb are used to define the system. An optimization procedure can be very helpful to reach a full exploitation of the potential benefit of CHP and solar systems.

The thermal and cooling storages which can be installed in each production unit or in the central unit can be modelled in the same way, accepting the approximations of perfect stratification of medium (water) inside the thermal storage. This approximation correspond to the hypothesis that, if the storage is not completely discharged, the residual energy is stored at the same temperature required by the DHN. The energy stored in the thermal energy storage, can be evaluated through:

$$\boldsymbol{Q_{ts}} = \boldsymbol{V_{ts}}\cdot\rho_p\cdot c_p\cdot\Delta t \tag{33}$$

As well as for the DHCN, the temperature difference Δt between inlet and outlet temperature is considered constant. Therefore, the thermal energy stored in the thermal storage is proportional to the volume of the medium inside the storage and it is considered as a decision variable. A set of equations is required to describe the energy balance of the thermal storage. In order to allow for the seasonal charging/discharging cycle, the thermal storage has to be modelled throughout the whole year, without any time decomposition as can be done for the other components, where a set of similar days can be represented by only one *typical day*. Applying the typical day approach to all operation variables, except for the variables which represent the energy stored in the thermal storages, allows us,

in any case, to reduce the overall number of variables, keeping the option of properly representing the charge and discharge phases of the thermal storages during all the year.

In the proposed model, the year is decomposed into 24 typical days of 24 h, one typical working day and one typical non-working day each month. Therefore, each single month is made up of four similar weeks, in turn made up of five similar working days and two similar non-working days. In this way, the optimal operation of the system is similar in each working or non-working day of the month and each month of the year is made up of 28 days. This approximation can be accepted selecting particular typical days which describe the whole year producing the same total consumption. Specific procedures for the identification of the proper typical days can be found in [31,32].

The energy balance of the thermal storage is approximated considering that the energy contained in the storage in a general time interval t is equal to the energy stored in the time interval t-1 multiplied by a thermal loss coefficient plus the input energy in the time interval t:

$$\boldsymbol{Q_{ts}}(m,s,d,r,h,u) - K_{los,ts}(u)\cdot\boldsymbol{Q_{ts}}(m,s,d,r,h-1,u) = \boldsymbol{H_{ts}}(m,d,h,u) \quad (34)$$

Additional constraints have to be added to connect the storage's condition at the end of a time period with that at the beginning of the following one. For example, Equation (35) connects two days of the same kind (some adjustment has to be introduced to take into account the transition from a working day, to a non-working day, or between different weeks, months, etc.):

$$\boldsymbol{Q_{ts}}(m,s,d,r,h,u) - K_{los,ts}(u)\cdot\boldsymbol{Q_{ts}}(m,s,d,r-1,24,u) = \boldsymbol{H_{ts}}(m,d,h,u) \quad (35)$$

Finally, the heat stored inside the storage $\boldsymbol{Q_{ts}}$, has to be lower than storage size $\boldsymbol{S_{ts}}$:

$$\boldsymbol{Q_{ts}}(m,s,d,r,h,u) \le \boldsymbol{S_{ts}}(u) \quad (36)$$

2.5. Energy Balances

Energy balances are a set of constraints which ensure that in each node and in each time interval the input energy is equal to the output energy. With reference to the superstructure represented in Figure 1, there are nodes three for each site (electric, thermal and cooling) plus the two nodes of the central site (electric and thermal). The energy balance of the network is included in the node energy balance. In the following the electric balance for a site u is described in detail, while the thermal and cooling balances are reported with no description.

The electricity and the thermal balances of a site are expressed by:

$$\begin{aligned}\boldsymbol{E_{ice}}(m,d,h,u) + \boldsymbol{E_{mgt}}(m,d,h,u) + E_{pvp}(m,d,h,u) + \boldsymbol{E_{bgt}}(m,d,h,u) = E_{cc}(m,d,h,u)\\ + E_{hp}(m,d,h,u) + E_{dem}(m,d,h,u) + \boldsymbol{E_{sol}}(m,d,h,u)\end{aligned} \quad (37)$$

$$\begin{aligned}H_{mgt}(m,d,h,u) + H_{ice}(m,d,h,u) + H_{stp}(m,d,h,u) + \boldsymbol{H_{boi}}(m,d,h,u) + H_{hp}(m,d,h,u)\\ +\boldsymbol{H_{net}}(m,d,h,v,u)\cdot(1-p_t\,(v,u)) = \boldsymbol{H_{ts}}(m,d,h,u) + H_{abs}(m,d,h,u) + H_{dem}(m,d,h,u) + \boldsymbol{H_{net}}(m,d,h,u,v)\end{aligned} \quad (38)$$

The thermal energy to be stored can be produced only by ICE, MGT and ST panels:

$$H_{mgt}(m,d,h,u) + H_{ice}(m,d,h,u) + H_{stp}(m,d,h,u) - \boldsymbol{H_{ts}}(m,d,h,u) \ge 0 \quad (39)$$

The cooling balance of a site is expressed by:

$$\boldsymbol{C_{abs}}(m,d,h,u) + \boldsymbol{C_{cc}}(m,d,h,u) + C_{hp}(m,d,h,u) = C_{dem}(m,d,h,u) + \boldsymbol{C_{ts}}(m,d,h,u) \quad (40)$$

The cooling energy to be stored can be produced only by CC, ABS and HP:

$$\boldsymbol{C_{abs}}(m,d,h,u) + \boldsymbol{C_{cc}}(m,d,h,u) + C_{hp}(m,d,h,u) - \boldsymbol{C_{ts}}(m,d,h,u) \ge 0 \quad (41)$$

As far as the central unit is concerned, the electricity produced by the central CHP can only be sold, while the thermal balance is expressed by:

$$H_{ice,c}(m,d,h) + \boldsymbol{H_{boi,c}}(m,d,h) + H_{stp,c}(m,d,h) = \boldsymbol{H_{net,c}}(m,d,h) + \boldsymbol{H_{ts,c}}(m,d,h) \quad (42)$$

The thermal production of the central unit can be shared among the users, which receive heat from the DHN through node u. Therefore, the thermal balance related to the central unit site reads:

$$\begin{aligned} H_{mgt}(m,d,h,u) + H_{ice}(m,d,h,u) + H_{stp}(m,d,h,u) + \boldsymbol{H_{boi}}(m,d,h,u) + H_{hp}(m,d,h,u) + \boldsymbol{H_{net}}(m,d,h,v,u)\cdot(1 - p_t\,(v,u)) \\ + \boldsymbol{H_{net,c}}(m,d,h)\cdot(1 - p_{t,c}) = \boldsymbol{H_{ts}}(m,d,h,u) + H_{abs}(m,d,h,u) + H_{dem}(m,d,h,u) + \boldsymbol{H_{net}}(m,d,h,u,v) \end{aligned} \quad (43)$$

All continuous variables have to be greater than zero, except the variables related to the thermal storage input/output heat flow ($\boldsymbol{H_{ts,c}}$, $\boldsymbol{H_{ts}}$, $\boldsymbol{C_{ts}}$) which are free. Positive values represent input flows, while negative values mean an energy extraction from the thermal storage. The temperatures of the thermal flows are not taken into account because it would have compromised the linearity of the problem. However, this is not a strong approximation considering that the thermal energy required by the users is normally supplied at a temperature of 50–55 °C and all components are able to produce the thermal energy at higher temperatures. Some restrictions due to the coupling of components related to the operating temperatures (ICE, MGT together with ABS) have been considered through a particular conformation of the superstructure and with additional constraints which consider this matter (e.g., Equations (17) and (18)).

2.6. Objective Functions

The economic objective function to be minimized is the total annual cost for owning, operating and maintaining the whole system:

$$Min:\ c_{tot} = c_{inv} + c_{man} + c_{ope} \quad (44)$$

The annual cost for the investment (c_{inv}) is the sum of the investment cost of the sites, of the central unit, and of the network. The investment cost of a site can be evaluated through:

$$\begin{aligned} c_{inv,u}(u) = \Sigma_j\,[f_{mgt}\cdot\boldsymbol{X_{mgt}}(j,u)\cdot c_{mgt}(j,u) + f_{ice}\cdot\boldsymbol{X_{ice}}(j,u)\cdot c_{ice}(j,u) + f_{hp}\cdot\boldsymbol{X_{hp}}(j,u)\cdot c_{hp}(j,u) + f_{abs}\cdot\boldsymbol{X_{abs}}(j,u)\cdot c_{abs}(j,u)] \\ + f_{boi}\cdot\boldsymbol{S_{boi}}(u)\cdot c_{boi} + f_{cc}\cdot\boldsymbol{S_{cc}}(u)\cdot c_{cc} + f_{pvp}\cdot S_{pvp}(u)\cdot c_{pvp} + f_{stp}\cdot\boldsymbol{S_{stp}}(u)\cdot c_{stp} + f_{ts}\cdot\boldsymbol{S_{ts}}(u)\cdot c_{ts} + f_{ts}\cdot\boldsymbol{S_{cs}}(u)\cdot c_{ts} \end{aligned} \quad (45)$$

The investment cost of the central unit is:

$$\begin{aligned} c_{inv,c} = f_{ice}\ (\boldsymbol{S_{ice,c}}\cdot c_{ice,v} + \boldsymbol{X_{ice,c}}\cdot c_{ice,f}\ ) + f_{boi}\cdot(\boldsymbol{S_{boi,c}}\cdot cboi,v + \boldsymbol{X_{boi,c}}\cdot cboi,f) \\ + fstp\cdot\boldsymbol{S_{stp,c}}\cdot cstp,c + fts\cdot\boldsymbol{S_{ts,c}}\cdot cts,c + fnet\cdot(cnet,f,c\cdot\boldsymbol{X_{net,c}} + cnet,v,c\cdot\boldsymbol{S_{H,net,c}}) \end{aligned} \quad (46)$$

The investment cost of the network is:

$$c_{net} = f_{net}\cdot\Sigma_{u,v}[c_{net,f,c}(1)\cdot(\boldsymbol{X_{tp}}(u,v) + \boldsymbol{X_{cp}}(u,v)) + c_{net,f,c}(1)\cdot\boldsymbol{X_{net}}(u,v) + c_{net,v}\cdot(\boldsymbol{S_{H,net,c}}(u,v) + \boldsymbol{S_{C,net}}(u,v))] \quad (47)$$

Maintenance costs related to the components are considered proportional to the products, while the operation costs include the costs for fuel, electricity bought from the grid and the eventual income from the sale of electricity. For each site u the annual operation cost is evaluated as:

$$\begin{aligned} c_{ope,u}(u) = \Sigma_{m,d,h}\,[c_{fue,chp}(m)\cdot(F_{ice}(m,d,h,u) + F_{mgt}(m,d,h,u)) + c_{fue,boi}(m)\cdot F_{boi}(m,d,h,u) \\ + c_{el,bgt}(m,d,h)\cdot\boldsymbol{E_{bgt}}(m,d,h,u) - c_{el,inc}\cdot E_{pvp}(m,d,h,u) - c_{el,sol}(m,d,h)\cdot\boldsymbol{E_{sol}}(m,d,h,u)]\cdot wgt(m,d,h) \end{aligned} \quad (48)$$

For the central site the annual operation cost is:

$$cope,c = \Sigma_u[cfue,ice,c\cdot Fice,c(m,d,h) + c_{fue,boi}(m)\cdot F_{boi,c}(m,d,h) - c_{el,sol}(m,d,h)\cdot\boldsymbol{E_{ice,c}}(m,d,h)]\cdot wgt(m,d,h) \quad (49)$$

The other objective function to be minimized is the annual operation greenhouse emissions (CO_2 emissions). The total annual emissions are related to the net electric energy received from the grid (bought minus sold) and to the fuel consumption by the DG energy system (boilers and/or CHP). Therefore, the total annual emissions can be evaluated through:

$$\begin{aligned} em_{tot} = em_{el} \cdot \Sigma_{\mathrm{m,d,h,u}} \left[\boldsymbol{E_{bgt}}(m,d,h,u) - \boldsymbol{E_{sol}}(m,d,h,u) - \boldsymbol{E_{ice,c}}(m,d,h) \right] \cdot wgt(m,d,h) \\ + emf,chp \cdot \Sigma_{\mathrm{m,d,h,u}} \left[F_{ice}(m,d,h,u) + F_{mgt}(m,d,h,u) \right] \cdot wgt(m,d,h) + emf,boi \cdot \Sigma_{\mathrm{m,d,h,u}} \left[(F_{boi}(m,d,h,u) \right. \\ \left. + F_{boi,c}(m,d,h) \right] \cdot wgt(m,d,h) + em_{f,cen} \cdot \Sigma_{\mathrm{m,d,h}} F_{ice,c}(m,d,h) \cdot wgt(m,d,h) \end{aligned} \quad (50)$$

The greenhouse emissions due to the consumption of fuel by the DG system are mainly related to the kind of fuel itself [33], while the electricity carbon intensity largely depends on the technology mix of each electricity supplier.

These two objectives are conflicting ones because the adoption of environmental efficient energy systems are costly. Likewise, the solution which allows the minimum annual cost does not permit us to obtain minimum total annual operation emissions.

The ε-constrained method [34] has been adopted to obtain the Pareto front solutions. First, the economic and environmental optimal solutions have been obtained. Secondly, the difference between the environmental objective in the two optimal cases has been calculated. Thirdly, a set of predefined intermediate emission levels has been identified and each level has been introduced as an additional constraint, in a further economic optimization. In this way, a set of dominant solutions, on the Pareto front of the multi-objective optimization (economic and environmental), can be obtained.

3. Case Study

A systematic approach for the selection of an appropriate DG energy supply system requires a detailed knowledge of heat, cooling, and electricity user demands. The detail level affects the model complexity and one of the factors which plays against the model compactness is the number of time intervals considered. These time periods are defined by the number of different energy demands that have to be covered, and the periodicity considered in the model (hourly, weekly, monthly). Long time periods, such as weeks or months, can be considered for industrial applications, characterized by quite constant energy demands that are fairly independent of environmental conditions. Hourly energy demand data is very important when tertiary sector/residential energy systems are analysed, where the influence of environmental conditions is quite important. In this last case, one solution to contain the model complexity is to represent the whole year through some typical days [32]. In the current optimization case study, the whole year has been subdivided into 24 typical days made up of 24 h each: 12 typical days refer to working days, while the remaining 12 refer to non-working days, so that each month is represented by one working and one non-working day. All values related to each single time interval are weighted through the parameter *wgt*, which consider their weights in the overall year. The grouping through typical days can be done for all variables, with the exception of the variables related to the thermal storages (either thermal or cooling) for which the whole year has to be considered (detailed explanation can be found in Section 2).

This case study is made up of nine tertiary sector users located close to each other in the centre of a small city (60,000 inhabitants) in the northeast of Italy. The users considered are all owned by the public service and this gave us the possibility to access the energy demand data. The users considered are the town hall, a theatre, a library, a primary school, a retirement home, the archive, a hospital, a secondary school and a swimming pool (Figure 2).

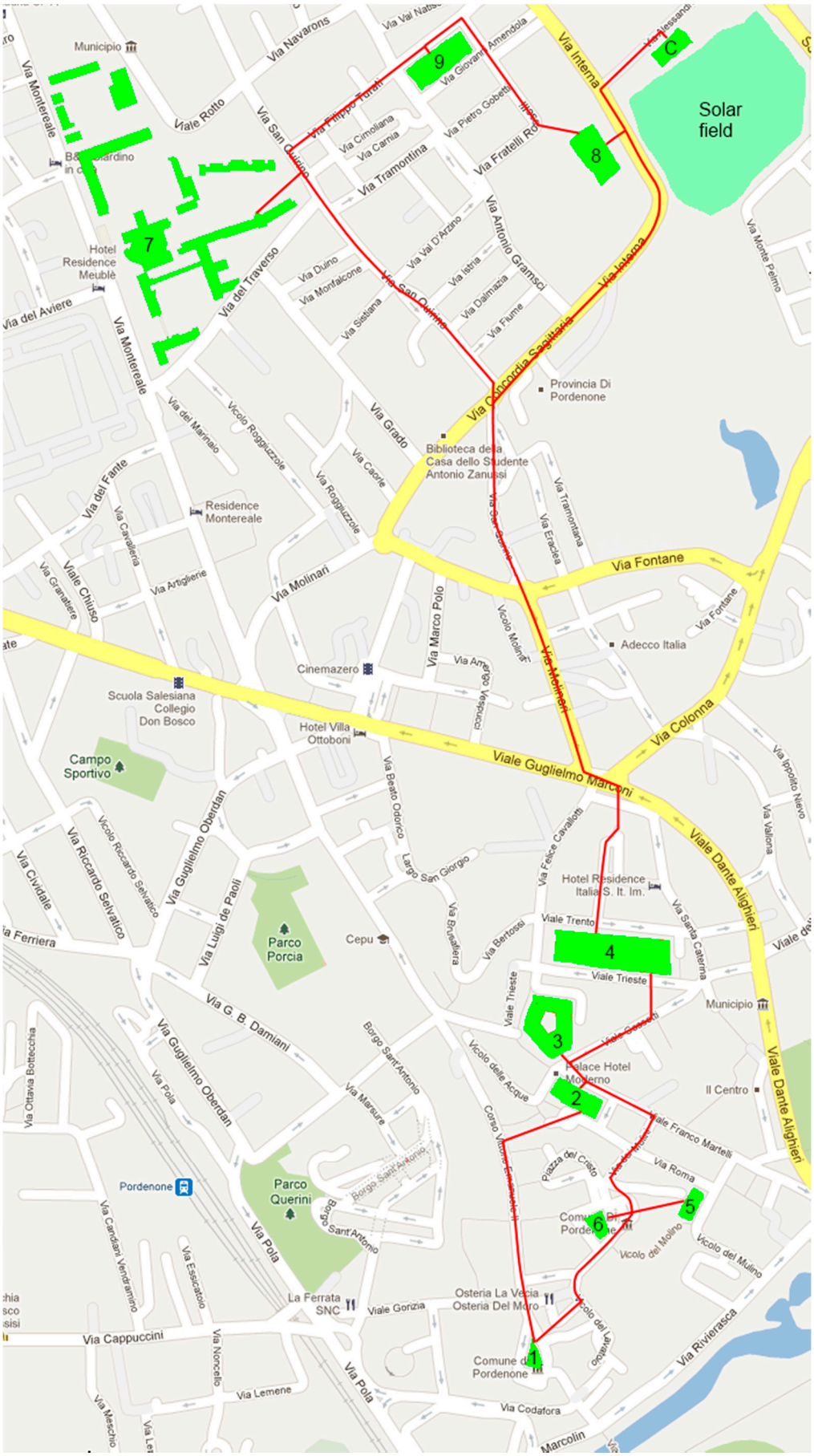

Figure 2. Plan of the possible path of the DHCN. 1—town hall; 2—theatre; 3—library; 4—primary school; 5—retirement home; 6—archive; 7—hospital; 8—school; 9—swimming pool; C—central unit site.

The heterogeneous choice of the buildings under consideration, characterized by different kinds of energy demands, allows us to consider the achieved results not affected by a specific user profile. Furthermore, a similar mix of users is expected to be easily recognized in a lot of other small and medium-sized towns in Europe.

Figure 2 shows the location of the nine buildings involved in the study and of the central unit together with solar field. In addition, the possible path of the DHCN is outlined in red.

The determination of the possible paths is the result of a preliminary study which considers:

- layout of the roads which connect the buildings;
- position of the underground utilities (waterworks, sanitation, gas network, etc.); and
- location of the boiler rooms of the buildings.

The users are close to each other and the maximum distance, between user 1 and the central unit, is about 2.5 km.

The users considered require thermal energy for space heating and for sanitary hot water, which is conventionally produced by boilers. The thermal energy for space heating is required at a temperature of about 65–70 °C. The cooling energy is required only for space cooling typically during the summer season and it is produced by compression chillers. In the optimizations, the design values of the temperatures for the operation of the DHN and DCN have been fixed at 70 °C and 12 °C, respectively. At the moment, the electric energy is bought from the grid and covers both the electricity demands and the electricity required to power the mechanical chillers.

Table 1 reports the annual energy consumptions and peak power of the nine users. The hospital requires about 50% of the electric energy consumption, the second energy consumer is the swimming pool, while the other users require less than 7% each. Similar situations can be found for thermal and cooling demand, with the exception that cooling energy is not required by the schools, as in summer there are no students and the cooling plants have not been provided. The last row of Table 1 shows the sum of all power peaks, and is, as can be expected, greater than the total power peak by about 10%. The electric demand shown in the table does not account for the energy required by the compression chillers for the production of cooling energy.

Table 1. User energy demand data.

	ELECTRIC		HEATING		COOLING	
USERS	**Year Dem.**	**Peak Power**	**Year Dem.**	**Peak Power**	**Year Dem.**	**Peak Power**
	(MWh)	(kWe)	(MWh)	(kWt)	(MWh)	(kWc)
Town Hall	346,640	189	692,720	410	148,712	150
Theatre	852,208	270	908,648	655	457,688	458
Library	492,240	110	587,608	296	112,364	115
Primary School	73,808	54	979,468	591	0	0
Retirement Home	489,048	101	739,956	246	207,568	138
Archive	82,516	36	429,604	238	78,652	91
Hospital	3,284,416	628	7,884,141	1847	1,445,612	2087
Secondary School	303,668	148	2,301,980	2084	0	0
Swimming Pool	1,043,572	315	2,794,580	1425	297,416	435
Total	6,968,116	1717	17,318,705	7017	2,748,012	3048
User Peak Power sum		1851		7792		3474

Figure 3 shows the trend of electric, thermal and energy demands for all buildings. It shows clearly that the trends are characteristic of tertiary sector users and also of a typical European continental climate, where during winter the thermal demand is higher than in summer period because of the need for space heating. During summer the thermal demand is only due to hot sanitary water demand, while there is a requirement of cold for space cooling. The electric energy is slightly higher during winter and lower in summer. This trend is related to the daylight hours, as during the summer there is a lower need of lighting.

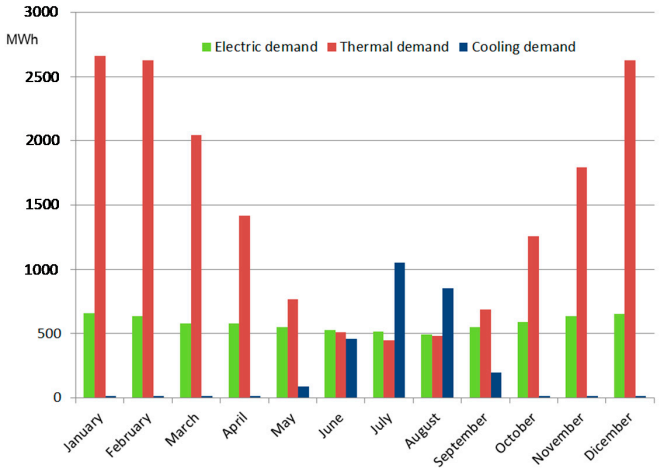

Figure 3. Trends of electric, thermal and cooling energy demands.

The energy demand patterns of the hospital in winter and summer are shown in Figure 4, for two representative working days. The winter trend shows greater electric energy demand during the daylight hours due to a higher occupancy factor, a heating demand higher in the morning and in the evening and a very low cooling demand, which is required by the air conditioning system. In summer, the cooling demand is higher compared with the winter season and reaches a maximum at about 3 p.m., the electric demand is similar to that of winter, while the thermal demand employed as sanitary water is higher during daylight hours and lower during the night. Each building has different energy patterns which depend on the occupancy factor, thermal insulation, night lighting, etc.

Figure 4. Hospital hourly energy demand patterns for a typical working day in winter (**top**) and summer (**bottom**).

The type and the size of the equipment which is part of the system superstructure must be appropriate to allow their integration, and proportionate to the user energy demands. All components considered in the optimization are commercially available and the prices have been obtained through a market survey. Two different kinds of components have been considered: fixed size components and variable size components. The optimal size/configuration of the energy system is obtained by defining the number of fixed size equipment installed and the size of variable size components (boilers, compression chillers, thermal storages).

Table 2 shows the sizes of components which can be installed in the different units. These sizes have been chosen consistently with the peak demand expected for each units (Table 1) taking into account that up to six elements of the same kind can be adopted in parallel. The technical characteristics of all pieces of equipment are described in File S1, jointly with their investment costs. The latter have been obtained by a market survey and also include transportation, installation, connection, engineering costs, etc.

Table 2. Component sizes (kW).

Equipment	Unit 1	Unit 2	Unit 3	Unit 4	Unit 5	Unit 6	Unit 7	Unit 8	Unit 9
MGT	65	100	30	30	30	30	200	65	100
ICE	70	140	50	50	50	50	200	70	140
ABS	70	105	35	35	35	35	105	70	105
HP	70	105	35	35	35	35	105	70	105

The amortization factors which multiply the investment costs are a function of the interest rate and of the life span of each component. The interest rate is assumed equal to 6% and is a sum of the real economic interest rate (4%) and a risk rate, assumed in this case equal to 2%. The life span of DHCN has been fixed equal to 30 years, for PV and ST panels and TS equal to 20 years, for ICE, MGT, ABS and HP equal to 15 years, and for BOI and CC equal to 10 years.

Maintenance costs are reported in File S1 and they are proportional to the energy produced by each component.

Operation costs are related to the costs of fuels and electricity. The Italian gas and electricity market has been liberalized since 2007, after a process which began in the 1999 with the "Bersani Decree" [35] and lasted eight years. Since 2007 all consumers can freely choose a supplier and leave the regulated-rate system or can remain connected to the old regulated market. Herein, the regulated-rate system has been considered as reference for the electricity and gas prices. The natural gas cost has been considered constant all year long, as well as the price of the bought electricity, while the price of the sold electricity has been assumed variable in each time interval, based on the hourly market prices. In particular, the bought electricity price has been considered equal to 0.17 €/kWh, while electricity sold price variable between 0.05–0.12 €/kWh, and natural gas price equal to 0.06 €/kWh. The prices considered include the pure cost of energy (about 40%) and taxes (about 60%).

The CO_2 emissions related to the consumption of electricity and natural gas have been assumed from literature [33]. The natural gas CO_2 emissions depend on the chemical composition of the gas and then on its provenience. However, the slight difference can be ignored considering the same value for the natural gas CO_2 emissions. The same approximation cannot be made for electricity. In fact, electricity carbon intensity depends heavily on the national electricity system. The reference case study has been optimized assuming the average electricity carbon intensity of the European Union in 2007–2009 (0.356 $kgCO_2/kWh$), while a second set of optimizations has been performed assuming the average electricity carbon intensity of the OECD Americas (Canada, United States, Mexico, Chile) in 2007–2009 (0.485 $kgCO_2/kWh$). The natural gas carbon intensive has been assumed equal to 0.202 $kgCO_2/kWh$.

To take into account the incentives that many European countries have adopted to promote the development of new energy technologies, two different incentives have been considered for the reference case study:

- natural gas detaxation for cogeneration use; and
- renewable energy production incentives.

Cogeneration systems complying with restrictions defined by the Dlgs 20/07 [36] are classified in Italy as "high efficiency cogeneration systems" and can operate with natural gas detaxation. Therefore, the cost of the natural gas for cogeneration use in the case study has been considered equal to 0.045 €/kWh (25% less compared with the conventional price of natural gas).

The second incentive considered in the case study is applied to the electricity produced by renewable energy sources. The rates considered in the case study for electricity produced by PV panels are 0.199 €/kWh if put in the grid and 0.111 €/kWh if directly used by the user, in line with Italian "Quinto Conto Energia" [37].

4. Results of the Optimizations

The aim of the optimization is to determine the optimal configuration of a complex DG energy system together with the optimal operational strategy on an hourly basis throughout one year. The objective functions of the optimizations are the total annual cost for owing, operating and maintaining the whole system and the total annual operation CO_2 emissions. Using the ϵ-constrained method the Pareto fronts have been obtained for different plant configurations.

The model has been optimized to obtain the optimal solution in 5 cases, corresponding to different district integration options:

1. conventional solution;
2. isolated solution;
3. distributed generation solution without central unit and district cooling network;
4. distributed generation solution with central unit but without cooling network; and
5. complete distributed generation solution.

As can be noted, the last configuration includes all the other configurations, while the conventional solution is a subset of all the other configurations. In this way it is possible to understand which is the influence of the different configurations and how they contribute to the achievement of the minimization of the objective functions.

The MILP model has been implemented in the X-press® Optimization Suite. X-press® is a commercial software produced by FICO® (Fair Isaac Corporation, San Jose, CA, USA) for solving large optimization problems by means of the application of resident algorithms. The mathematical model has been implemented through Mosel, a modelling and programming language that allows users to formulate problems, to solve them by using the solver engines, and to analyse the solutions.

The optimization toolbox uses evolutionary algorithms, cut generations and heuristic algorithms, together with the branch and bound technique and revised simplex techniques. The branch and bound method starts with the optimization of the relaxed MILP problem, and explores the solution tree step by step, by fix one discrete decision variable at a time. In this way, the absolute optimal value of the objective function is not generally obtainable without exploring the complete solution tree, and a near optimal solution has to be accepted, stopping the optimization when a determined gap between the objective function of the relaxed problem and that of the current problem is reached. The case study has to be considered a very large problem as there are about 600,000 decision variables and 950,000 constraints. For this reason, the optimization procedure is stopped when a gap lower than 1% is reached.

The optimizations have been performed with a PC equipped with an Intel® processor Core™ i7CPU 920@2.67 GHz, 6.00 GB RAM and a 64 bit operating system. An optimization of the overall problem, accepting a gap of 1%, takes about 100 h.

4.1. Conventional Solution

The Conventional Solution is considered as the reference solution, assuming that all thermal energy is produced by BOI, all cooling energy is produced by electric CC and all electricity is bought from the grid. Furthermore, the thermal and cooling energy can be stored in separated energy storages. The optimization is performed adopting a reduced superstructure where only BOI and CC can be installed (Figure 5).

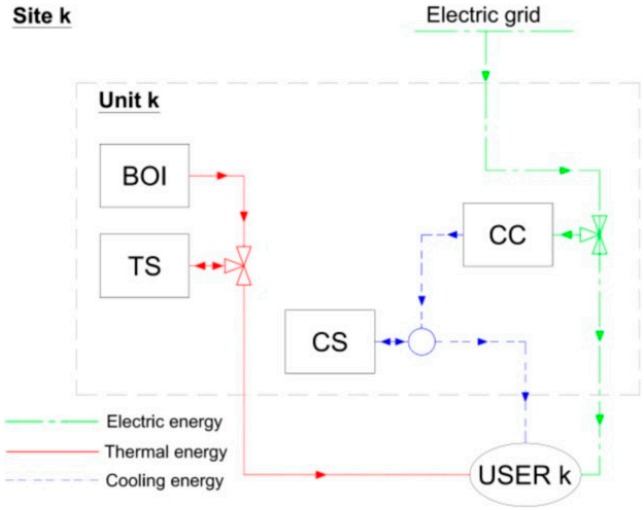

Figure 5. Superstructure of the conventional solution.

Table 3 shows the optimal configuration of the conventional solution, obtained by minimizing the total annual cost. The table reports the energy peaks of each single user. It can be noted that the boilers installed in each unit are of smaller sizes compared with the thermal peaks, as all units are provided with a proper sized thermal storage. On the other hand, the sizes of the compression chillers correspond to the cooling peaks as the cooling storages are not included in the optimal solution.

Table 3. Optimal configuration of the conventional solution.

User	1	2	3	4	5	6	7	8	9
Electric Peak (kW)	189	270	110	54	101	36	628	148	315
Thermal Peak (kW)	410	655	296	591	246	238	1847	2084	1425
Cooling Peak (kW)	150	458	115	0	138	91	2087	0	435
Boiler (kW)	294	479	217	418	205	179	1623	1673	1153
Comp. Chiller (kW)	150	458	115	0	138	91	2087	0	435
Thermal storage (kW)	544	375	312	766	173	298	690	2251	1564

Table 4 shows the economic and environmental results of the optimization performed for the conventional solution.

Table 4. Economic and environmental optimization of the conventional solution.

User	1	2	3	4	5	6	7	8	9	Total
Natural gas (k€/y)	44	58	37	62	47	27	498	146	177	1096
Electricity cost (k€/y)	67	171	90	13	95	18	640	52	194	1340
Operating cost (k€/y)	111	228	127	75	142	46	1138	198	371	2437
Maintenance cost (k€/y)	1	2	1	1	1	1	11	2	3	23
Total investment cost (k€/y)	58	141	43	33	47	35	597	127	188	1267
Annual investment cost (k€/y)	7	18	6	4	6	4	77	16	24	163
Total annual cost (k€/y)	**120**	**248**	**134**	**80**	**149**	**51**	**1226**	**216**	**399**	**2622**
Electricity emission (t/y)	141	358	189	26	199	39	1341	108	407	2807
Natural gas emission (t/y)	148	194	125	209	158	92	1677	492	596	3691
Total annual emission (t/y)	**289**	**551**	**314**	**236**	**356**	**130**	**3018**	**600**	**1003**	**6497**

The total annual cost of the conventional solution is 2622 k€ per year, and it is made up of about 93% of operation costs (costs for thermal energy and electricity), 6% of investment costs and 1% of maintenance costs. The results show also that the hospital contributes to the total annual cost by about 50%, as it is the largest energy consumer. The table shows also the environmental results and that they depend basically on the energy consumption of each user. The energy balances are reported in Table 5. The thermal energy produced by BOI is slightly higher than the thermal energy required by the users, because of the heat losses in the TS. It should also be noticed that, as can be expected, the thermal and cooling energies produced by the components are all used by the users without any waste.

Table 5. Optimal annual energy magnitudes (MWh)—conventional solution.

User	1	2	3	4	5	6	7	8	9	Total
Bought Electricity (MWh)	396	1005	530	74	558	109	3766	304	1143	7884
Electricity user demand (MWh)	347	852	492	74	489	83	3284	304	1044	6968
Electricity required by CC (MWh)	50	153	37	0	69	26	482	0	99	916
Heat produced by BOI (MWh)	696	911	590	984	741	432	7888	2312	2802	17,357
Thermal user demand (MWh)	693	909	588	979	740	430	7884	2302	2795	17,319
Wasted heat (MWh)	0	0	0	0	0	0	0	0	0	0
Cooling energy by CC (MWh)	149	458	112	0	208	79	1446	0	297	2748
Cooling energy user demand (MWh)	149	458	112	0	208	79	1446	0	297	2748
Wasted cooling energy (MWh)	0	0	0	0	0	0	0	0	0	0

The results presented in this section, and obtained by minimizing the economic objective function of the conventional solution, will be used as a reference for the evaluation of the forthcoming optimizations.

4.2. Isolated Solution

Two different superstructures have been considered for the optimization of the isolated solution: one including all components considered in Figure 6 and another including all those components, with the exception of the local thermal storages (either heating or cooling). These two different optimizations allow us to understand what the influence of the thermal storages in the optimal solution is. Pure economic and environmental optimizations have been conducted for the isolated solutions.

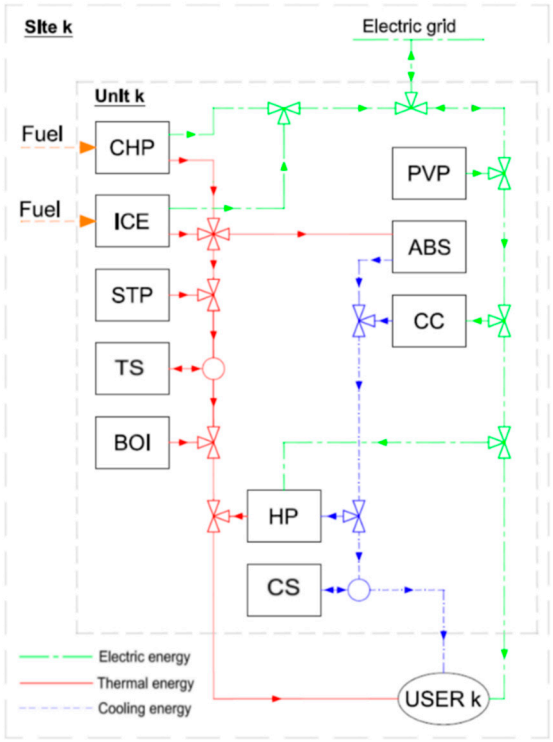

Figure 6. Superstructure of the isolated solution with TSs.

The optimal configurations of the isolated solutions are compared to each other and to the conventional solution in Table 6. For matters of clarity, only the total power installed, for each kind of component, has been reported. Focusing on the economic optimizations, the ICEs have been adopted as cogenerators, while the MGTs are never installed. The ST panels are never adopted as well, because PV panels are more convenient and the space intended for the installation of both kind of panels is limited.

Table 6. Optimal configurations of the isolated solutions compared to the conventional solution.

	Economic Optimization			Environmental Optimization	
	Conventional Solution	**Isolated Solution without TS**	**Isolated Solution**	**Isolated Solution without TS**	**Isolated Solution**
ICE (kW)	0	2820	2840	4920	4920
MGT (kW)	0	0	0	3900	3900
BOI (kW)	6241	2145	984	609	431
ABS (kW)	0	840	735	3570	3570
HP (kW)	0	1750	980	3570	3570
CC (kW)	3474	1274	1763	1948	2008
PV panels (kW)	0	225	225	45	0
ST panels (m^2)	0	0	0	1438	1800
TS (kWh)	6973	0	15,016	0	36,000
CS (kW)	0	0	0	0	36,000

The introduction of the TS allows a measurable reduction of the sizes of BOI and HP. The CS are not adopted in the optimal solution but, due to the arrangement of the optimal operation caused by the availability of the TS, the ABSs size decreases while the CCs size has to increase, in order to satisfy the cooling peak demand. Focusing on the environmental optimization, it should be observed that the adoption of large components does not imply any penalty for the environmental objective

function. However, it can be outlined that the ST panels replace the PV panels adopted in the economic optimization.

Table 7 shows the results of the optimizations performed for the isolated solutions. Comparing the economic optimizations to the conventional solution, the cost for natural gas used by BOIs significantly decreases, as well as that of the bought electricity. The cost for natural gas used by CHP did not exist for the conventional solution. However, the operating cost in the optimal isolated solutions is halved compared with the conventional one. The optimal isolated solutions, without and with the TS and CS, obtained minimizing the economic objective functions allow us to reduce the total annual cost by 36.7% and 38.8%, and the total annual emissions by 15.9% and 16.5%, respectively. Therefore, the adoption of TSs allows us to reduce either the total annual cost or the total annual emissions.

Table 7. Total economic and environmental results of the optimizations—isolated solutions.

	Economic Optimization			**Environmental Optimization**	
	Conventional Solution	**Isolated Solution without TS**	**Isolated Solution**	**Isolated Solution without TS**	**Isolated Solution**
CHP natural gas cost (k€/y)	0	1458	1561	624	600
BOI natural gas cost (k€/y)	1096	67	50	13	2
Buoght electricity cost (k€/y)	1340	29	28	1216	1257
Sold electricity income (k€/y)	0	365	490	138	140
Photovolatic incentive (k€/y)	0	68	68	16	0
Operating cost (k€/y)	2437	1121	1081	1699	1720
Maintenance cost (k€/y)	23	120	128	53	52
Total investment cost (k€/y)	1267	4288	4021	12,138	12,518
Annual investment cost (k€/y)	163	421	395	1175	1206
Total annual cost (k€/y)	**2622**	**1661**	**1604**	**2927**	**2977**
Reduction wrt conv. solution		**36.7%**	**38.8%**	**−11.6%**	**−13.5%**
Electricity emissions (t/y)	2807	61	59	2545	2633
Sold electricity emissions (t/y)	0	1363	1806	508	499
Natural gas emissions (t/y)	3691	6769	7173	2844	2701
Total annual emissions (t/y)	**6497**	**5467**	**5427**	**4882**	**4836**
Reduction wrt conv. solution		**15.9%**	**16.5%**	**24.9%**	**25.6%**

The environmental optimization shows an increase of the operation costs of about 60% compared with the economic optimizations, while it allows a reduction of about 25% of the total annual emissions with respect to the conventional solution. It can be also noted that the amount of emissions due to electricity usage significantly increases, while the emissions saved due to the electricity sold to the grid, and that in consequence of natural gas usage, significantly decrease.

The energy balances of the optimizations performed for the isolated solutions are reported in Table 8. It can be observed that the bought electricity is negligible in the economic optimizations, while a significant amount of electricity is sold to the grid. The latter is higher when the TSs are adopted, as they allow us to decouple the thermal demand from the electric one, and to operate the ICE when it is more convenient. Almost all thermal demand is satisfied by the ICEs, while the cooling demand is covered by all three kinds of components which can be adopted (CC, ABS, HP). In the environmental optimizations, the quantity of electricity produced by CHPs and sold to the grid decreases noticeably, while the quantity of electricity bought from the grid increases. The heat produced by the HPs increases significantly, while the cooling energy required by the users is produced by CCs and HPs.

Table 8. Total optimal annual energy magnitudes (MWh)—isolated solutions.

	Economic Optimization			Environmental Optimization	
	Conventional Solution	**Isolated Solution without TS**	**Isolated Solution**	**Isolated Solution without TS**	**Isolated Solution**
ICE electricity	0	11,563	12,455	4599	4591
MGT electricity	0	0	0	331	175
PV panels electricity	0	239	239	48	0
Bought electricity	7884	173	166	7150	7395
Electric user demand	6968	6968	6968	6968	6968
CC electricity	916	137	191	398	394
HP electricity	0	1042	628	3337	3399
Sold electricity	0	3828	5073	1426	1,4012
ICE thermal energy	0	16,906	18,133	6603	6628
MGT thermal energy	0	0	0	566	299
BOI thermal energy	17,357	1064	787	205	36
HP thermal energy	0	2103	946	9279	9419
ST panels thermal energy	0	0	0	1108	1387
Thermal user demand	17,319	17,319	17,319	17,319	17,319
ABS thermal energy	0	1733	1604	290	131
Wasted thermal energy	0	1022	399	152	92
CC cooling energy	2748	410	574	1194	1182
ABS cooling energy	0	1127	1055	163	79
HP cooling energy	0	1213	1121	1392	1488
Cooling energy demand	2748	2748	2748	2748	2748
Wasted cooling energy	0	2	1	0	0

4.3. Distributed Generation Solution

The distributed generation solution is obtained by adding the DHN to the isolated solution (Figure 7). The thermal energy produced in a production unit can be used directly either by the user of the site, or by other users, exchanging the heat through the DHN. This solution gives the opportunity to create a central production unit where all energy is produced and sent to the users through the DHN. The electric energy, if not used directly to the user has to be sent to the electric network. However, the isolated solution would still be adopted if it were more convenient, based on economic, or environmental evaluations.

Table 9 shows the optimal configurations obtained for the distributed cogeneration solution. As previously introduced, the Pareto front of the bi-objective optimization has been identified by means of the ε-constraint method, by fixing the pollution levels at the 30%, 60% and 90% of the difference between the two environmental objectives of the economic and environmental optimal solutions.

Table 9. Optimal configurations of the distributed generation solution.

	Environmental Opt.	**90% Env. Opt.**	**60% Env. Opt.**	**30% Env. Opt.**	**Economic Opt.**
DHN pipes (n°)	18	13	9	7	7
ICE (kW)	1920	2190	2290	2590	28,403,900
MGT (kW)	3900	0	0	0	0
BOI (kW)	502	0	0	0	0
ABS (kW)	3570	0	0	595	770
HP (kW)	3570	2590	2380	1715	1050
CC (kW)	1593	1682	1759	1620	1656
PV panels (kW_p)	0	0	134	225	225
ST panels (m^2)	1800	1800	734	0	0
TS (kWh)	36,000	6316	8553	12,337	15,017
CS (kWh)	36,000	0	0	0	0

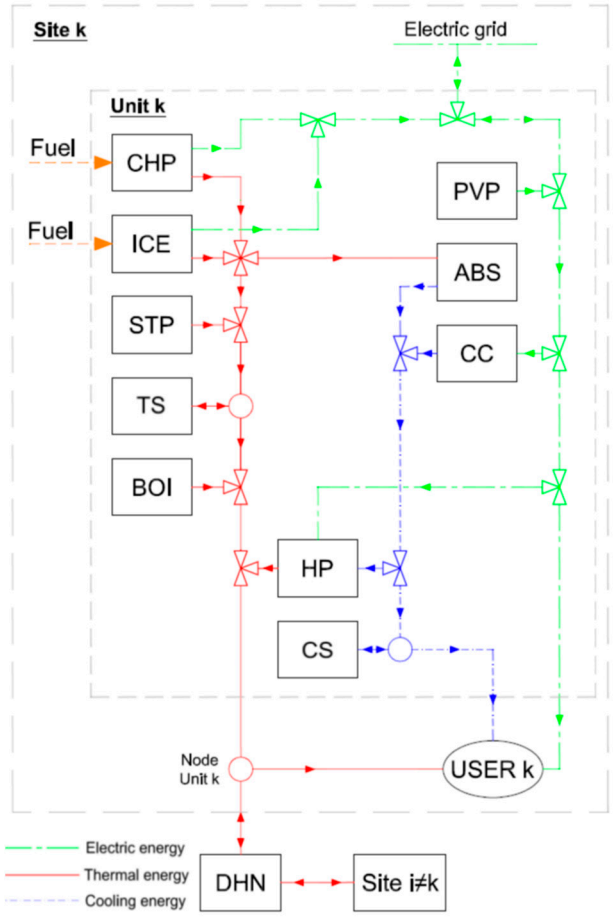

Figure 7. Superstructure of the distributed generation solution.

From a general overview of Table 9, it can be noted that the DHN is convenient either from an economic or environmental point of view, while the MGTs, the CSs and the BOIs are actually never adopted, with the exception of the Environmental optimum.

Moving from the economic towards the environmental optimal solution, the number of the DHN pipelines increase, as well as the size of the HPs and the ST panels installed. The size of the CCs remains quite constant while the size of ICEs, of ABSs, of PV panels and of TSs adopted decreases. The sizes of the components related to the environmental optimal solution do not follow this trend, because the size of the components is free of penalty.

Figure 8 shows the Pareto front of the distributed generation solutions, and is compared with the isolated solutions and conventional solution. It can be clearly seen that, with the exception of the environmental optimal solutions, all the other optimal solutions dominate the conventional solution and allow both the objective functions to be improve. However, the distributed generation solution does not lead to a significant improvement of the economic objective function, compared with the Isolated Solutions (less than 1%).

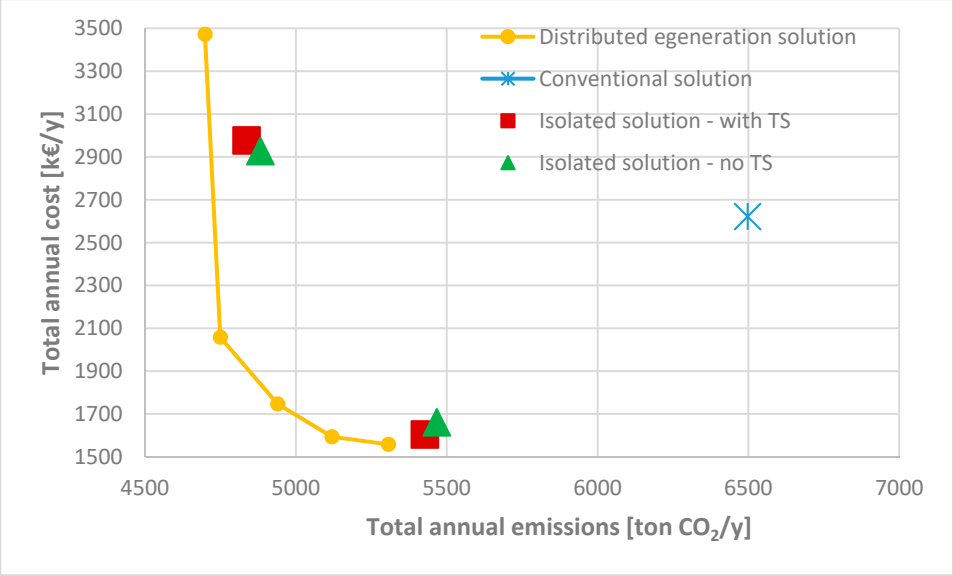

Figure 8. Pareto front of the optimal distributed generation solutions, including the points representing isolated solutions (with and without TS) and the conventional solution.

Table 10 shows the economic and environmental results of the optimizations. Moving from the economic to the environmental optimum the operation cost increase by about 80%, resulting from a significant increase of the bought electricity cost and a reduction of the natural gas cost and sold electricity income. The maintenance cost decreases noticeably, while the investment cost increases significantly. The environmental optimal solutions are characterized by a noticeable reduction of the total annual emissions, but a raise in total annual cost.

Table 10. Total economic and environmental results of the optimizations—distributed generation solutions.

	Environmental Optimization	90% Env. Optimization.	60% Env. Optimization.	30% Env. Optimization.	Economic Optimization.
CHP natural gas cost (k€/y)	389	643	994	1296	1614
BOI natural gas cost (k€/y)	0	0	0	0	0
Buoght electricity cost (k€/y)	1603	1030	446	130	21
Sold electricity income (k€/y)	76	82	126	264	539
Photovolatic incentive (k€/y)	0	0	30	58	67
Operating cost (k€/y)	1917	1591	1284	1105	1028
Maintenance cost (k€/y)	37	57	84	107	132
Annual investment cost (k€/y)	1519	410	378	381	397
Total investment cost (k€/y)	17,422	4403	3968	4050	4178
Total annual cost (k€/y)	**3472**	**2058**	**1746**	**1593**	**1558**
Reduction wrt conv. solution	**−32.44%**	**21.52%**	**33.42%**	**39.23%**	**40.59%**
Electricity emissions (t/y)	3358	2157	934	273	44
Sold electricity emissions (t/y)	269	292	456	972	1981
Natural gas emissions (t/y)	1710	2885	4461	5818	7244
Total annual emissions (t/y)	**4699**	**4750**	**4940**	**5120**	**5307**
Reduction wrt conv. solution	**27.68%**	**26.89%**	**23.97%**	**21.20%**	**18.33%**

Table 11 shows the total optimal annual energy magnitudes for the different solutions. Moving from the economic towards the environmental optimal solution, it can be noted that the electricity produced by the ICEs decreases significantly. On the other hand, the electricity bought from the grid increases to feed electric components, such as CCs and HPs. In the economic optimal solution, the thermal energy produced by ICEs satisfies almost completely the demand, while it decreases significantly in the environmental optimal solution and is partially replaced by the thermal production of HPs and ST panels. As far as the cooling energy balance is concerned, the production of the

CCs is quite constant, while ABSs and HPs have opposite trends, moving from economic towards environmental optimum. The HPs result more suitable in the environmental optimal solution. In all optimal solutions, the thermal and cooling wasted energy is negligible.

Table 11. Total optimal annual energy magnitudes (MWh)—distributed generation solutions.

	Environmental Optimization	90% Env. Optimization	60% Env. Optimization	30% Env. Optimization	Economic Optimization
ICE electricity	3131	5190	8014	10,341	12,933
MGT electricity	0	0	0	0	0
PV panels electricity	0	0	141	239	239
Bought electricity	9431	6060	2625	767	123
Electric user demand	6968	6968	6968	6968	6968
CC electricity	217	230	266	180	231
HP electricity	4617	3232	2266	1560	532
Sold electricity	760	820	1281	2729	5565
ICE thermal energy	4619	7468	11,510	15,022	18,742
MGT thermal energy	0	0	0	0	0
BOI thermal energy	0	0	0	0	3
HP thermal energy	11,581	8663	5406	3450	834
ST panels thermal energy	1387	1387	566	0	0
Thermal user demand	17,319	17,319	17,319	17,319	17,319
ABS thermal energy	0	0	0	809	1704
Wasted thermal energy	0	0	0	0	9
CC cooling energy	652	689	797	540	692
ABS cooling energy	0	0	0	523	1140
HP cooling energy	2096	2059	1951	1686	917
Cooling user demand	2748	2748	2748	2748	2748
Wasted cooling energy	0	0	0	0	1

If two (or more) objectives are considered, the choice of the proper configuration has to be based on further technical evaluation of the designer and on an economic evaluation of the stakeholders. If the only aim is to achieve the lowest total annual cost, the economic optimal solution will be adopted, but in a different context, where the sensitivity to environmental problems is more important, the 90% environmental solution could be chosen. It allows the total annual emissions to be significantly reduced, controlling, at the same time, the Total annual cost.

In this specific case study, the 60% environmental optimal solution has been identified as the proper compromise. Figure 9 shows the optimal configuration and the lay out of the network in this case. This solution provides a subdivision of the DHN into two different subsystems: the first one is made up of sites 1–6, the second one is made of the sites 7–9. In the first subsystem the site 2 can be identified as a central node, where the greatest part of the thermal energy is produced and sent to the other sites through the DHN. In the second subsystem the sites are integrated with each other and a main site cannot be identified.

Distributed generation solutions allow a slight improvement of the economic objective function (less than 1%) to be achieved, jointly with an improvement of the environmental one of about 2%, compared with the isolated solutions.

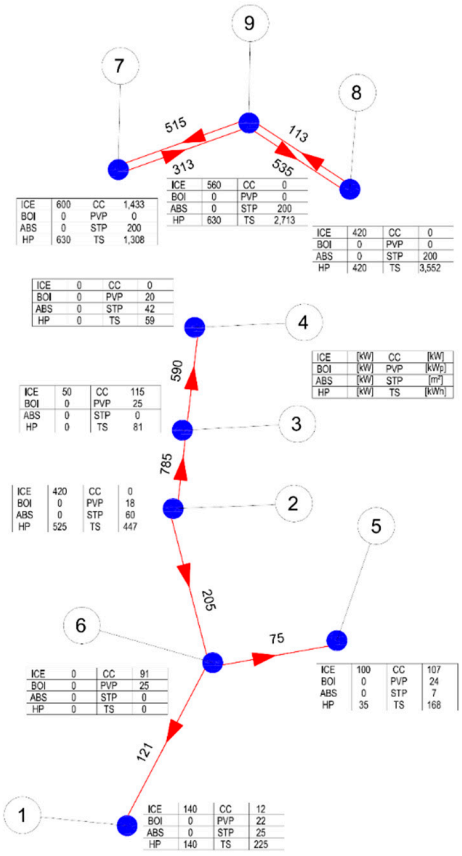

Figure 9. Optimal DHN of the 60% environmental optimum—distributed generation solution. In red the DHN pipes have been reported together with their size (kW). The tables report the size of the components installed.

4.4. Distributed Generation Solution Integrated with the Central Solar System

The following results have been obtained by considering a superstructure which embeds all components included in the previous one, but a central system has been added, made up by an ICE, a BOI, the central storage and the solar field (Figure 10).

Four optimizations have been performed: one economic optimization, one environmental optimization and two intermediate optimizations, obtained constraining the environmental objective function. Looking at the optimal configurations (Table 12) it can be noted that in all optimizations the solar field is adopted together with the central thermal storage, while the central BOI is not adopted because it is not economic to produce energy in the central unit and then transfer it to the sites, losing thermal energy through the DHN. Neither is the ICE is adopted, because the marginal cost of the heat results to be much higher when the electricity is sold to the grid (and therefore it has a low value) compared with the situation when the electricity is directly used by the users. Therefore, as the electric energy produced by the central ICE cannot be sent directly to the users, but can only be sold to the grid, the adoption of the central ICE is not economic.

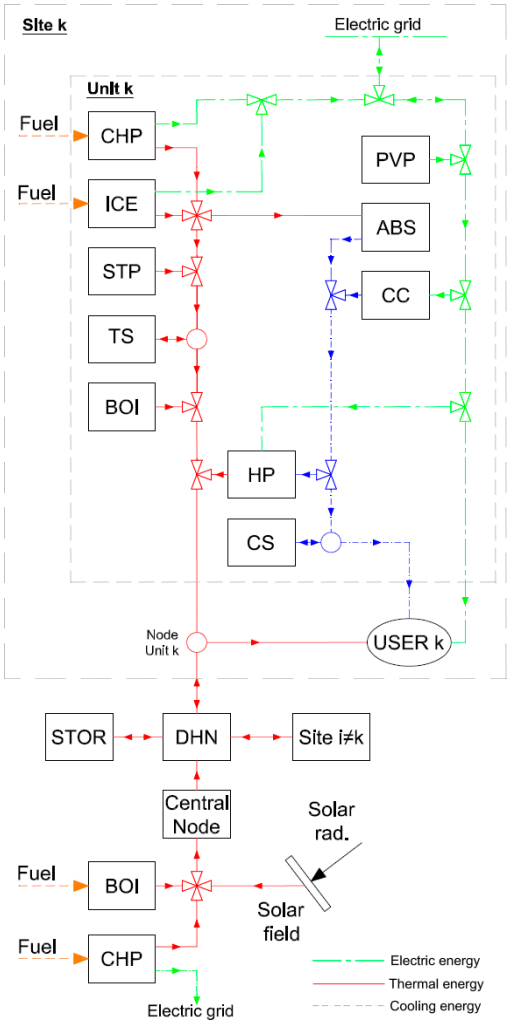

Figure 10. Superstructure of the distributed generation solution integrated with central solar unit.

Table 12. Optimal configurations of the distributed generation solutions Integrated with central solar unit.

	Environmental	70% Env.	30% Env.	Economic
	Opt.	**Opt.**	**Opt.**	**Opt.**
DHN pipes [n°]	14	8	7	7
Central pipe size (kW)	7500	6323	3579	1907
ICE (kW)	4920	1840	2380	2500
MGT (kW)	0	0	0	0
BOI (kW)	3480	3408	2730	2023
ABS (kW)	3570	1260	1155	1085
HP (kW)	3570	1120	1225	1155
CC (kW)	1584	1056	1053	1233
PV panels (kW*p*)	225	225	225	225
ST panels (m^2)	0	0	0	0
TS (kWh)	0	0	2315	5134
CS (kWh)	0	0	0	0
Central ICE (kW)	0	0	0	0
Central BOI (kW)	0	0	0	0
ST field (m^2)	27,736	23,585	19,013	8035
Central TS (kWh)	400,000	173,935	41,855	19,025

A difference to be highlighted concerning the previous section is the presence of the boilers to cover the thermal peaks, the size of which increases as we move towards the environmental solution.

A separation in the DHN is still present in the economic and 30% environmental optimizations, forming two separated subsystems: sites 1–6, and sites 7–9, with the second group only connected to the central unit. Starting from the 70% environmental optimization, all users are connected to each other, whilst the storages installed in the local production units disappear, replaced by a larger central thermal storage, with lower heat loss. In parallel, the solar thermal field increases threefold compared with the economic optimum. The size of ABSs increases, too, while the ST panels at the user site are never adopted.

Table 13 shows the economic and environmental results of the optimizations. The trends of the costs and of the emissions are similar to the ones observed in the previous optimizations. Comparing Table 10 with Table 13, it can be observed that the operating cost of the solutions integrated with the central solar system is lower (−6%), while they are characterized by higher investment costs (+30%). It is worth noting that the Pareto front obtained with integrating the central solar system (Figure 11) dominates the other Pareto fronts, as all the solutions obtained allow lower annual costs together with lower annual emissions to be achieved.

Table 13. Total economic and environmental results of the optimizations—distributed generation solutions integrated with central solar unit.

	Environmental	**70% Env.**	**30% Env.**	**Economic**
	Opt.	**Opt.**	**Opt.**	**Opt.**
CHP natural gas cost (k€/y)	86	741	1059	1339
BOI natural gas cost (k€/y)	1	10	9	33
Buoght electricity cost (k€/y)	1482	451	221	32
Sold electricity income (k€/y)	30	125	234	373
Photovolatic cost (k€/y)	75	53	55	66
Operating cost (k€/y)	1464	1025	1000	965
Maintenance cost (k€/y)	10	63	88	113
Total investment cost [k€]	22,314	8248	6368	5359
Annual investment cost (k€/y)	1760	705	569	453
Total annual cost (k€/y)	**3233**	**1792**	**1657**	**1531**
Reduction wrt conv. solution	**−22.32%**	**31.64%**	**36.89%**	**41.61%**
Electricity emissions (t/y)	3104	945	463	67
Sold electricity emissions (t/y)	190	461	856	1385
Natural gas emissions (t/y)	388	3362	4748	6268
Total annual emissions (t/y)	**3301**	**3846**	**4392**	**4950**
Reduction wrt conv. solution	**49.20%**	**40.80%**	**32.41%**	**23.81%**

Table 14 shows the total annual energy magnitudes obtained for the optimizations of the distributed generation solution integrated with the central solar system. The trends of each item are similar to the ones observed in previous Table 11. The most important differences are the noticeable increase of the thermal production from the ST panels, and the greater amount of wasted thermal energy. They both are due to the presence of a large ST field, the production of which allows a great fraction of the thermal demand to be satisfied by renewable energy, but cannot be usefully exploited during all the year, even adopting the optimal operation strategy. In the pure and 30% economic optimizations, the solar field covers about 50% of the thermal demand and a small central thermal storage is adopted. It is operated with a daily/weekly charging/discharging cycles.

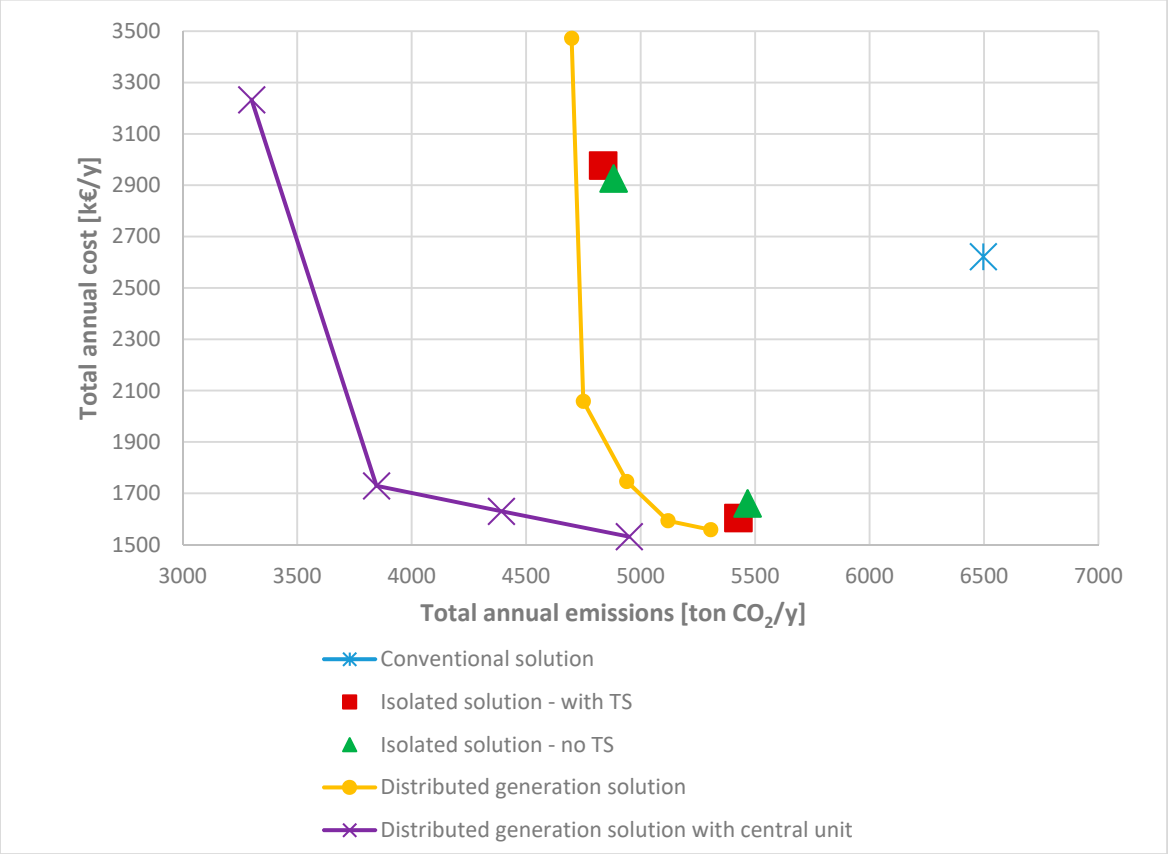

Figure 11. Pareto front of the optimal distributed generation solutions integrated with central solar system.

Table 14. Total optimal annual energy magnitudes (MWh)—distributed generation solutions integrated with the central solar system.

	Environmental	70% Env.	30% Env.	Economic
	Opt.	**Opt.**	**Opt.**	**Opt.**
ICE electricity	693	5957	8482	10,956
MGT electricity	0	0	0	0
PV panels electricity	239	239	239	239
Bought electricity	8718	2656	1302	188
Electric user demand	6968	6968	6968	6968
CC electricity	209	137	121	162
HP electricity	1938	453	529	363
Sold electricity	534	1294	2404	3889
ICE thermal energy	1024	8547	12,284	15,979
MGT thermal energy	0	0	0	0
BOI thermal energy	11	161	146	529
HP thermal energy	3991	675	866	497
ST panels thermal energy	20,931	17,880	14,651	6191
Thermal user demand	17,319	17,319	17,319	17,319
ABS thermal energy	0	2316	2336	2341
Wasted thermal energy	7850	6918	8018	2571
CC cooling energy	626	410	364	487
ABS cooling energy	0	1521	1522	1549
HP cooling energy	2122	820	872	717
Cooling user demand	2748	2748	2748	2748
Wasted cooling energy	0	3	10	4

During summer, when the solar field is producing a lot of thermal energy, the thermal storage is full, but the users do not require thermal energy, therefore, the heat produced by the solar field is wasted. If a larger thermal storage were adopted, it would imply an investment cost noticeably greater, which would not be paid back by the related savings. Hence, it is cheaper to waste the exceeding heat (instead of storing it) and produce it with boilers and/or cogenerators, when it is necessary.

Figure 12 shows the trends of the thermal energy demand of sites 7, 8 and 9, the central storage level and the in/out storage thermal flow in a typical week, operated following the economic optimal strategy. The other sites are not considered because the central storage is not connected to them. It can be noted that, during the weekend, the thermal demand is lower than during the working days, consequently the heat produced by the solar field is saved in the thermal storage. This heat is then used in the first hours of the following working days, when the operation of the ICE is not economic.

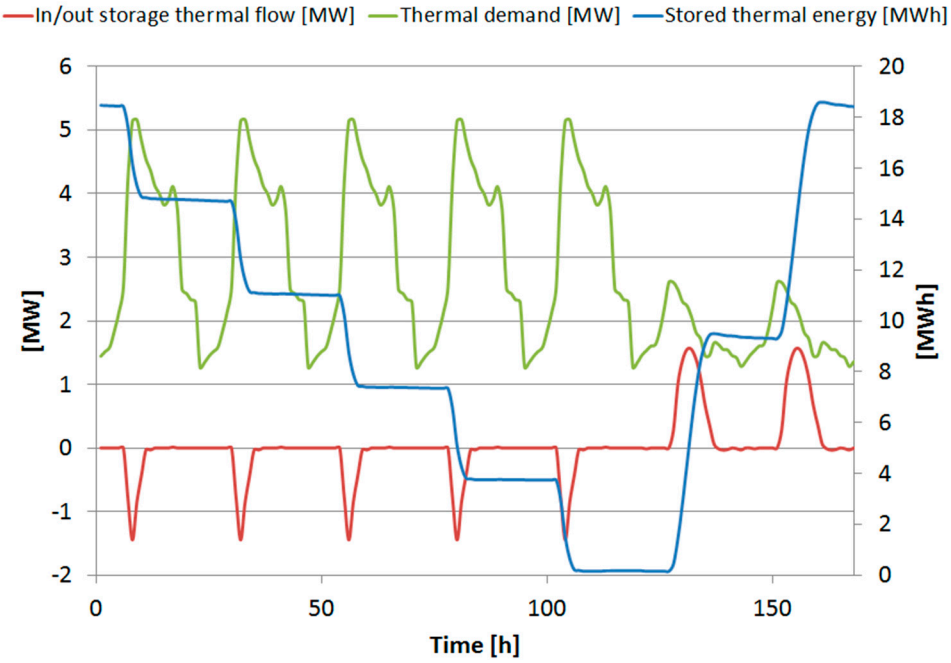

Figure 12. Optimal operation of the storage in a typical week-economic optimization of the distributed generation solutions integrated with the central solar system.

In the pure environmental and 70% optimizations, the solar field and the thermal storage are larger, compared with the other optimizations. In this case, the thermal storage is operated with a seasonal charging/discharging cycle: from April to August, part of the heat produced by the solar field is stored in the thermal storage, and is used from September to November. In the other months the storage is operated with weekly charging/discharging cycles (see Figure 13).

Larger thermal storage and solar field would probably allow a real seasonal operation of the storage: the heat stored from April to August would be used from September to March. However, this solution would have led to higher investment costs which would not have been paid back by a sufficient reduction of the operation costs.

Figure 13 shows the optimal operation of the storage, with charging/discharging cycles, for the 70% environmental optimization of the distributed generation solution integrated with the central solar system. The figure shows clearly that each month is characterized by weeks with the same operation, consistently with the time discretization adopted in the optimization model. In fact, the year is made up of 48 weeks (instead of 54) grouped by four, representing the 12 months. Each single week is made up of five working days plus two non-working days. Therefore, all weeks of the same month are characterized by the same operation.

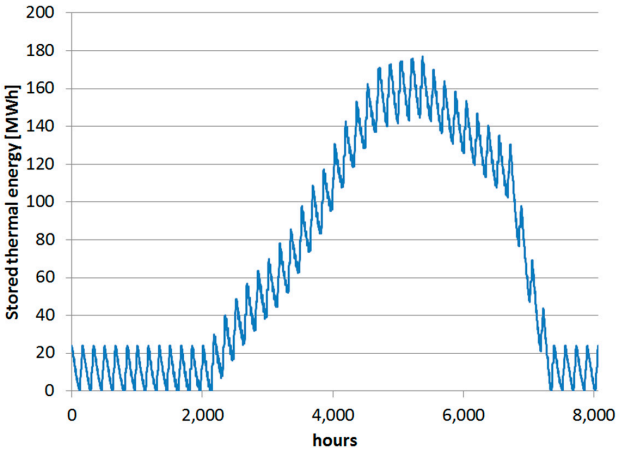

Figure 13. Yearly optimal operation of the storage−70% environmental optimization of the distributed generation solution integrated with the central solar system.

Additionally, in this case, a compromise between the best economic result and the most environmental friendly solution have been looked for on the Pareto front, and it has been identified with the 70% environmental optimal solution. It allows a total cost reduction by about 32% and a total annual emissions reduction by about 41%, compared with the conventional solution.

Figure 14 shows the optimal configuration and the lay-out of the network. It can be noted that the DHN connects the users to each other differently from the optimal solution shown in Figure 9, where the users were subdivided into two sub networks. In this case the thermal energy produced in the central unit can be sent to all the users through the DHN. The dimension of the pipes decreases moving towards sites 1 and 7. The introduction of the central solar field and of a large thermal storage, allows the solution shown in Figure 14 to obtain a noticeable reduction of the CO_2 emissions (−22%), compared to that shown in Figure 9.

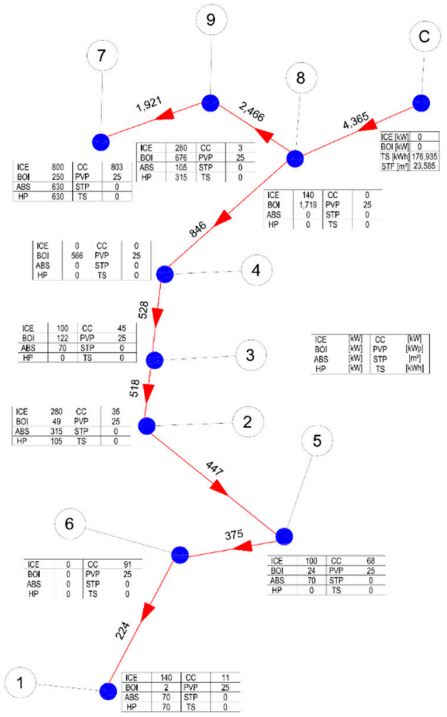

Figure 14. Optimal DHN of the 70% environmental optimum—distributed generation solution integrated with the central solar system. In red the DHN pipes have been reported together with their size (kW). The tables report the size of the components installed.

4.5. Complete Distributed Generation Solution

The complete distributed generation solutions include also the DCN into the superstructure and corresponds to the most general superstructure presented in Section 2 (see Figure 1).

Table 15 shows the optimal configuration of the four optimizations performed: economic, environmental and the two intermediate optimizations, obtained by constraining the environmental objective function. The optimal configurations and the trends are very similar to the ones obtained in the previous paragraph, where the DCN was not included in the superstructure.

Table 15. Optimal configurations of the complete distributed generation solutions.

	Environmental	**70% Env.**	**30% Env.**	**Economic**
	Optimization	**Opt.**	**Opt.**	**Optimization**
DHN pipes (n°)	14	8	7	7
DCN pipes (n°)	7	4	3	3
Central pipe size (kW)	7500	4980	4118	1922
ICE (kW)	4920	1840	2270	2380
MGT (kW)	0	0	0	0
BOI (kW)	12	1954	1406	1252
ABS (kW)	3570	1435	1190	1120
HP (kW)	3570	1890	1680	1680
CC (kW)	778	250	174	306
PV panels (kW*p*)	225	225	225	225
ST panels (m^2)	0	0	0	0
TS (kWh)	0	0	2176	4939
CS (kWh)	0	0	0	0
Central ICE	0	0	0	0
Central BOI	0	0	0	0
ST field (m^2)	22,736	21,764	17,664	8710
Central TS (kWh)	400,000	169,926	30,980	20,366

Also in this case, the first two optimizations (economic and 30% optimizations) subdivide the whole system in two sub-DHN: sites 1–6, and sites 7–9 connected to the central unit.

The last two optimizations (pure and 70%environmental optimizations) provide a DHN which connects all sites to each other. The DCN is adopted and always connects site 2 to sites 5 and 6, and site 9 to 7. Starting from the 70% environmental optimization, also site 1 is connected to site 6. Compared with the previous optimizations (see Table 12) the size of the CC decreases noticeable, because of the presence of the DCN.

The introduction of DCN does not affect significantly the economic and environmental performance of the system. In fact, an improvement of only a few percentage points is obtained for the annual cost and for the annual emissions (see Table 16), in comparison with the case considered in the previous paragraph. Focusing on the economic optimization, the operation costs decrease by about 60 k€. The annual investment cost increases by 10 k€, due to the adoption of the three pipes of the DCN. Thus, the total annual cost decreases by about 50 k€. The environmental optimization leads to a slight improvement of the total annual emissions (10 tons).

From Figure 15, it can be easily inferred that the complete distributed generation solutions dominates all the other solutions analysed for this case study. The economic optimal solution allows us to obtain a reduction by about 43% of the annual cost and by about 25% of the annual emissions (see Table 16), compared with the conventional solution. The environmental optimal solution allows a reduction of about 50% to be obtained, compare with the conventional solution, but the total annual cost increases. The corresponding performance of the 70% environmental solution, which has been identified as the best compromise among the complete distributed solutions, are a reduction of about 32% for the annual cost and of about 41% for the annual emissions.

Table 16. Total economic and environmental results of the optimizations—complete distributed generation solution.

	Environmental Optimization	70% Env. Opt.	30% Env. Opt.	Economic Optimization
CHP natural gas cost (k€/y)	202	757	1026	1242
BOI natural gas cost (k€/y)	0	7	4	33
Buoght electricity cost (k€/y)	1474	486	218	38
Sold electricity income (k€/y)	126	153	266	340
Photovolatic incentive (k€/y)	75	53	56	66
Operating cost (k€/y)	1475	1045	926	908
Maintenance cost (k€/y)	10	60	88	107
Total investment cost (k€/y)	24,806	8114	6909	5219
Annual investment cost (k€/y)	1611	680	592	466
Total annual cost (k€/y)	**3095**	**1785**	**1606**	**1481**
Reduction wrt conv. solution	**−18.05%**	**31.93%**	**38.75%**	**43.50%**
Electricity emissions (t/y)	3087	1018	457	80
Sold electricity emissions (t/y)	197	453	864	1157
Natural gas emissions (t/y)	403	3262	4769	5974
Total annual emissions (t/y)	**3292**	**3827**	**4362**	**4897**
Reduction wrt conv. solution	**49.33%**	**41.10%**	**32.87%**	**24.63%**

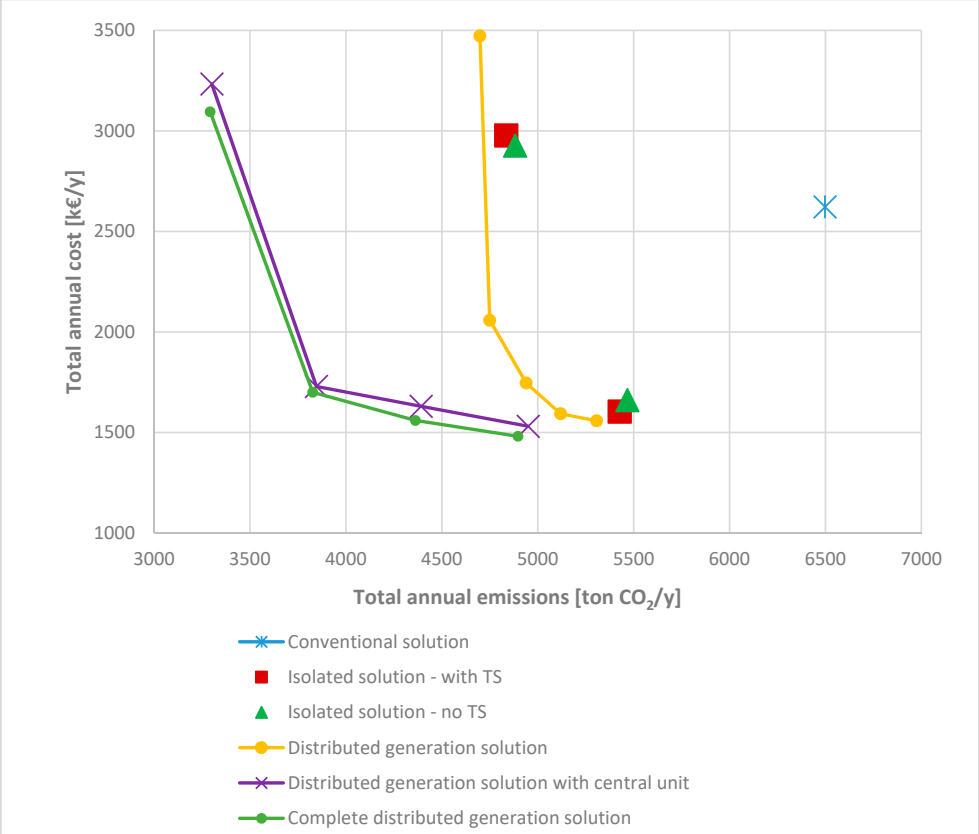

Figure 15. Pareto front of the optimal complete distributed generation solutions.

A comparison among the annual energy magnitudes of the economic optimizations for the complete distributed generation and for the distributed generation integrated with the central solar system (Tables 14 and 17) shows some differences, which highlight the effect of the DCN in the economic optimal solutions. The electricity used by the HPs and the cooling energy produced by the ABSs are higher by about 67% and 8%, respectively, when the DCN is adopted. At the same time, the sold electricity and the electrical consumption of the CC are lower by about 17% and 68%, respectively. Nevertheless, the additional operation options allowed by the adoption of the DCN do not lead us to a

strong improvement of the environmental, or of the economic performance of the system, but only small improvements by about 1% and 3%, respectively, are obtained.

Table 17. Total optimal annual energy magnitudes (MWh)—complete distributed generation solutions.

	Environmental	70% Env.	30% Env.	Economic
	Optimization	**Opt.**	**Opt.**	**Optimization**
ICE electricity	726	5807	8510	10,412
MGT electricity	0	0	0	0
PV panels electricity	239	239	239	239
Bought electricity	8671	2858	1283	226
Electric user demand	6968	6968	6968	6968
CC electricity	78	54	34	51
HP electricity	2035	610	604	607
Sold electricity	501	1257	2411	3234
ICE thermal energy	1057	8313	12,241	15,187
MGT thermal energy	0	0	0	0
BOI thermal energy	0	112	63	527
HP thermal energy	3974	820	916	1054
ST panels thermal energy	17,520	16,771	13,612	6711
Thermal user demand	17,319	17,319	17,319	17,319
ABS thermal energy	0	2077	2431	2560
Wasted thermal energy	4436	5930	6753	3439
CC cooling energy	234	162	101	153
ABS cooling energy	0	1377	1594	1676
HP cooling energy	2537	1227	1074	933
Cooling user demand	2748	2748	2748	2748
Wasted cooling energy	0	4	8	5

The evaluation of Pareto fronts of the multi-objective optimizations performed allows the best compromise between the minimum annual cost and the minimum annual emissions to be identified for each different heat/cooling integration options. Table 18 summarizes these compromise solutions and compares them with the economic optimum obtained for the conventional and isolated solutions.

Table 18. Summary of the different compromise solutions obtained for the different configurations considered.

	Conventional Solution	Isolated Solution	Distributed Generation Solution	Distributed Generation Solution with Central Unit	Complete Distributed Solution
DHN pipes (n°)	-	-	9	8	8
DCN pipes (n°)	-	-	-	-	4
Central pipe size (kW)	-	-	-	6323	4980
ICE (kW)	-	1840	2290	1840	1840
MGT (kW)	-	0	0	0	0
BOI (kW)	5241	984	0	3408	1954
ABS (kW)	-	735	0	1620	1435
HP (kW)	-	980	2380	1120	1890
CC (kW)	3474	1763	1759	1056	250
PV panels (kW*p*)	-	225	134	225	225
ST panels (m^2)	-	0	734	0	0
TS (kWh)	6973	15,016	8553	0	0
CS (kWh)	0	0	0	0	0
Central ICE	-	-	-	0	0
Central BOI	-	-	-	0	0
ST field (m^2)	-	-	-	23,585	21,764
Central TS (kWh)	-	-	-	173,935	169,926
Operating cost (k€/y)	2473	1080	1284	1025	1045
Total investment cost (k€/y)	1267	4020	3968	8248	8114
Total annual cost (k€/y)	**2622**	**1604**	**1746**	**1792**	**1785**
Reduction wrt conv. solution	**-**	**38.8%**	**33.4%**	**31.7%**	**31.9%**
Total annual emissions (t/y)	**6497**	**5427**	**4940**	**3846**	**3827**
Reduction wrt conv. solution	**-**	**16.2%**	**24.0%**	**40.8%**	**41.1%**

As mentioned before, the 70% environmental optimization has been identified as the best compromise for the Complete distributed solution. Figure 16 shows its optimal configuration: the layout of the DHCN is shown together with the size of the components installed in each site. The DCN connects sites 2, 5, 6 and 1, and a single pipe connects site 7 to 9. The layout of the DHN is very similar to the one shown in Figure 14 for the distributed generation solution integrated with the central solar system, while the component sizes installed in each production unit are slightly changed. These differences are consequence of the additional operation options allowed by the adoption of the DCN.

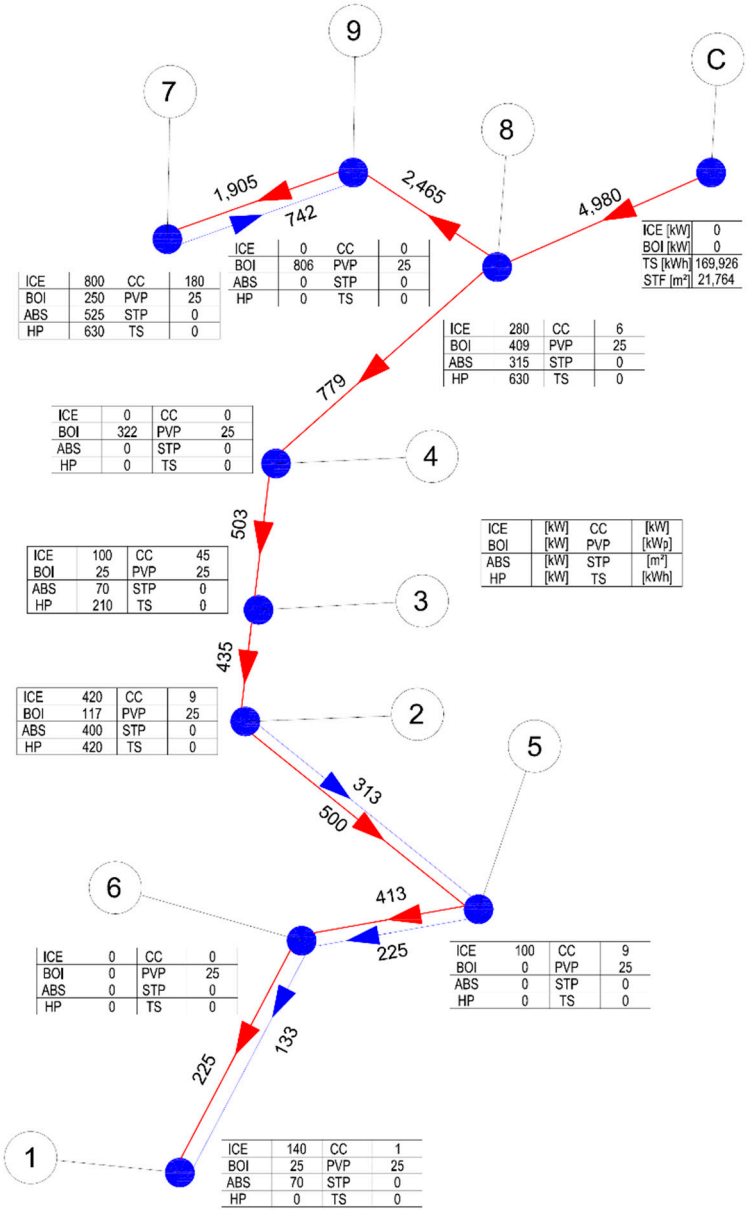

Figure 16. Optimal DHCN of the 70% environmental optimum—complete distributed generation solution. In red the DHN pipes and in blue the DCN pipes have been reported together with their size (kW). The tables report the size of the components installed.

Nevertheless, in the evaluation of the optimization results, we have to keep in mind that the MILP problems have been optimized with a gap equal to 1%. Therefore, two feasible solutions with a very low difference in the objective functions (in principle, lower than 1%) may be regarded by the optimization algorithm as equivalent, even if their decision variable vectors are different. When the DHCN is included in the superstructure, the number of similar solutions increases exponentially, and

solutions which have a different location, or size, of some components may result to be equivalent for the MILP algorithm, because of their similar optimal values of the objective functions.

5. Conclusions

The MILP model presented in this paper has been used to optimize the configuration and operation for a case study of a distributed generation system for heating and cooling in an urban area. The model allows us to obtain the optimal configuration of the system, satisfying the energy requirements of the users, that minimizes the total annual cost and the total CO_2 emissions during operation. The aim of the work is to compare on a common basis, different district heating integration options. In more detail, five cases have been considered:

- conventional solution;
- isolated solution;
- distributed generation solution without central unit and district cooling network;
- distributed generation solution with central unit but without cooling network; and
- complete distributed generation solution.

Starting from the conventional solution, the further cases consider, at each step, additional components and a more thorough district heating/cooling integration. The best solution, both from the economic or environmental points of view can be achieved with the complete distributed generation solution, which includes various kinds of energy components, a DHCN, a solar field and a seasonal thermal storage. The best economic solution allows a 43% reduction of the total annual cost compared with the conventional solution, while the best environmental solution allows about a 50% reduction of the total annual emissions (see Table 16). This result can be achieved only with the optimal size and/or multiplicity of the components and with the optimal operation of the energy system.

The economic optimization of the Isolated Solution, which comprises only the distributed cogenerators and absorption machines, without any district integration, permits a consistent reduction of the total cost compared with the conventional solution (37%), together with a reduction of the CO_2 emissions (16%). In this case, the adoption of local thermal storages is suggested from both the economic and environmental points of view). This performance is similar to the one obtained for the economic optimization of the complete distributed generation; the isolated solution also implies a much lower investment cost (Table 7). On the other hand, the complete distributed generation solution is cheaper in the long term view (over 20 years) and allows also a greater reduction of the annual emissions. In fact, important reductions of the annual emissions can be obtained only with the adoption of the solar field, of the seasonal storage and of the district heating network.

The distributed generation solution, with heating district integration, but without the solar field and the seasonal storage, permits us to slightly improve both the economic and the environmental objective functions (less than 2%) compared with the isolated solution. The further integrations of the DG system allow incremental benefit of similar magnitude for the economic optimal solutions (1–3% each), reaching the higher reduction with the complete distribution generation solution, as highlighted before.

From the analysis of the Pareto fronts obtained, it can be inferred that a very high environmental benefit (greater than 40%) can be obtained by complete distribution generation solution, without giving up a large long-term cost reduction of about 32% (see Table 18). At the same time, it is evident that the advantages obtained by introducing the cooling district network are very small, at least when the optimal synthesis and operation of the system is considered.

When the central solar field with central TS can be chosen, the optimal compromise solution adopts a central TS of about 172,000 kWh and a solar field of about 22,000 m^2. The optimal operations identified in this paper show that the central thermal storage is operated with seasonal charging/discharging cycles only when the environmental objective function is considered in the optimizations (Figure 13). The heat produced by the solar field during warmer months is used during the first colder months.

Meanwhile, pure economic optimizations provide a weekly operation of the central thermal storage: the heat produced by the solar field during week-end, when the energy demand is lower, is used during the following working days.

Supplementary Materials: The following are available online at http://www.mdpi.com/2076-3417/9/17/3521/s1: File S1.

Author Contributions: Research conceptualization: M.R. methodology: D.B. and M.R.; software development: D.B. and M.C.; result validation: D.B.; formal analysis: P.P.; case study investigation: M.C.; resources: P.P. and M.R.; data curation: D.B. and M.C.; writing—original draft preparation: P.P.; writing—review and editing: M.C.; supervision: P.P. and M.R.; funding acquisition: P.P. and M.R.

Funding: This research received no external funding

Conflicts of Interest: The authors declare no conflict of interest.

Nomenclature

δ_t	Thermal losses percentage
Δt	Difference between outlet and inlet temperatures (K)
$\eta_{boi,c}$	Central BOI efficiency
$\boldsymbol{\psi_{boi,c}}$	Additional variable for the centralized BOI
ρ_p	Medium density (Kg/m^3)
$\boldsymbol{\xi_{ice,c}}$	Additional variable for the centralized Internal Combustion Engine (ICE)
A_p	Diameter of the pipeline (m^2)
c	Central unit
$\boldsymbol{C_{abs}}$	Cold produced by the Absorption Chiller (ABS) (kWh)
c_{abs}	ABS investment cost (e)
c_{boi}	BOI investment cost (e)
$c_{boi,f}$	BOI fixed investment cost (e)
$c_{boi,v}$	BOI variable investment cost (e/kW)
$\boldsymbol{C_{cc}}$	Cold produced by the Compression Chiller (CC) (kWh)
C_{dem}	User cooling demand (kWh)
$c_{el,bgt}$	Electricity cost (e/kWh)
$c_{el,inc}$	Photo-voltaic panels (PV panels) incentive (e/kWh)
$c_{el,sol}$	Electricity income (e/kWh)
$c_{fue,boi}$	BOI fuel cost (e/kWh)
$c_{fue,chp}$	Combined Cooling Heat and Power (CHP) fuel cost (e/kWh)
$c_{fue,ice,c}$	Central ICE fuel cost (e/kWh)
c_{hp}	HP investment cost (e)
C_{hp}	Cold produced by the HP (kWh)
c_{ice}	ICE investment cost (e)
$c_{ice,f}$	ICE fixed investment cost (e)
$c_{ice,v}$	ICE variable investment cost (e/kW)
c_{inv}	Investment annual cost (e/y)
$c_{inv,c}$	Central unit annual investment cost (e/y)
$c_{inv,u}$	Site annual investment cost (e/y)
c_{man}	Maintenance annual cost (e/y)
c_{mgt}	Micro Gas Turbine (MGT) investment cost (e)
c_{net}	DHCN annual investment cost (e/y)
$c_{net,f,c}$	Fixed cost of the DHCN pipeline (e/m)
$c_{net,v}$	Variable cost of the DHCN pipeline (e/kW · m)
$c_{net,v,c}$	Variable cost of the central DHN pipeline (e/kW · m)
c_{ope}	Operating annual cost (e/y)

$c_{ope,c}$	Central unit annual operation cost (e/y)
$c_{ope,u}$	Unit annual operation cost (e/y)
c_p	Specific heat(Kj/kg K)
c_{pvp}	PV panels investment cost (e/m)
c_{stp}	Solar thermal panels (ST panels) investment cost (e/m^2)
$c_{stp,c}$	Central ST panels investment cost (e/m^2)
c_{tot}	Total annual cost (e/y)
$\boldsymbol{C_{ts}}$	Cooling energy storage input (kWh)
c_{ts}	Thermal Storage (TS) investment cost (e/kWh)
$c_{ts,c}$	Central TS investment cost (e/kWh)
d	Generic day
$\boldsymbol{E_{bgt}}$	Electricity bought from the network (kWh)
E_{cc}	Electricity required by the CC (kWh)
$\boldsymbol{E_{hp,c}}$	Electricity required by the HP when producing cold (kWh)
E_{dem}	User electricity demand (kWh)
$\boldsymbol{E_{hp,h}}$	Electricity required by the HP when producing heat (kWh)
E_{hp}	Electricity required by the HP (kWh)
$\boldsymbol{E_{ice}}$	Electricity produced by the ICE (kWh)
$\boldsymbol{E_{ice,c}}$	Electricity produced by the centralized ICE (kWh)
$E_{ice,lim}$	ICE operation limits (kW)
em_{el}	Electricity carbon intensity (kgCO_2/kWh)
$em_{f,boi}$	BOI fuel carbon intensity (kgCO_2/kWh)
$em_{f,cen}$	Central CHP fuel carbon intensity (kgCO_2/kWh)
$em_{f,chp}$	CHP fuel carbon intensity (kgCO_2/kWh)
$\boldsymbol{E_{mgt}}$	Electricity produced by the MGT (kWh)
em_{lim}	Emission limit in the s-constrained optimization (kgCO_2/kWh)
em_{tot}	Total annual CO_2 emissions (kg)
E_{pvp}	Electricity produced by the PV panels (kWh)
$\boldsymbol{E_{sol}}$	Electricity sold to the network (kWh)
f_{abs}	ABS amortization factor (y^{-1})
F_{boi}	Fuel required by the BOI (kWh)
f_{boi}	BOI amortization factor (y^{-1})
$F_{boi,c}$	Fuel required by the central BOI (kWh)
f_{cc}	CC amortization factor (y^{-1})
f_{hp}	HP amortization factor (y^{-1})
F_{ice}	Fuel required by the ICE (kWh)
f_{ice}	ICE amortization factor (y^{-1})
$F_{ice,c}$	Fuel required by the centralized ICE (kWh)
F_{mgt}	Fuel required by the MGT (kWh)
f_{mgt}	MGT amortization factor (y^{-1})
f_{net}	DHCN amortization factor (y^{-1})
f_{pvp}	PV panels amortization factor (y^{-1})
f_{stp}	ST panels amortization factor (y^{-1})
f_{ts}	TS amortization factor (y^{-1})
h	Generic hour
H_{abs}	Heat required by the ABS (kWh)
$\boldsymbol{H_{boi}}$	Heat produced by the BOI (kWh)
$\boldsymbol{H_{boi,c}}$	Heat produced by the central BOI (kWh)
$H_{boi,lim,c}$	Centralized BOI operation limits (kW)
H_{dem}	User thermal demand (kWh)
H_{hp}	Heat produced by the HP (kWh)
H_{ice}	Heat produced by the ICE (kWh)

$H_{ice,c}$	Heat produced by the centralized ICE (kWh)
H_{mgt}	Heat produced by the MGT (kWh)
$\boldsymbol{H_{net}}$	Thermal energy transferred through the pipeline (kWh)
$\boldsymbol{H_{net,c}}$	Thermal energy transferred through the pipeline of the central DHN (kWh)
$H_{net,lim}$	Size limits of the pipelines (kWh)
H_{stp}	Solar panel thermal production
$H_{stp,c}$	Centralized solar field thermal production
H_{ts}	Thermal energy storage input (kWh)
$H_{ts,c}$	Thermal energy storage input (kWh)
j	Generic component
k	Generic site/user
Kf_{ice}	ICE Performance curve linearization coefficient
$Kf_{ice,c}$	Centralized ICE Performance curve linearization coefficient
Kh_{ice}	ICE Performance curve linearization coefficient
$Kh_{ice,c}$	Central ICE performance curve linearization coefficient
K_{hp}	HP Performance curve linearization coefficient
$K_{los,ts}$	Percentage thermal loss coefficient
K_{pv}	Unitary PV production
K_{stp}	Unitary solar thermal production
l_p	Length of the pipeline (m)
m	Generic month
$\boldsymbol{O_{boi,c}}$	Central BOI operation (binary)
$\boldsymbol{O_{hp,c}}$	HP cold operation (binary)
$\boldsymbol{O_{hp,h}}$	HP heat operation (binary)
$\boldsymbol{O_{ice}}$	ICE operation (binary)
$\boldsymbol{O_{ice,c}}$	Centralized ICE operation (binary)
p_t	Pipeline thermal loss per unit length (km^{-1})
$p_{t,c}$	Pipeline thermal loss per unit length of the central DHN pipeline (km^{-1})
$\dot{Q}_p$	Heat transferred by a DHCN pipeline (kWh)
$\boldsymbol{Q_{ts}}$	Thermal energy stored in a thermal storage (kWh)
s	Generic week
$\boldsymbol{S_{boi}}$	BOI size (kW)
$\boldsymbol{S_{boi,c}}$	Central BOI size (kW)
$S_{boi,lim,c}$	Central BOI size limits (kW)
$\boldsymbol{S_{cc}}$	CC size (kW)
$\boldsymbol{S_{C,net}}$	Size of the cooling pipeline (kW)
$\boldsymbol{S_{cs}}$	Cooling storage size (kWh)
$\boldsymbol{S_{H,net}}$	Size of the thermal pipeline (kW)
$\boldsymbol{S_{H,net,c}}$	Size of the central DHN pipeline (kW)
$S_{hp,lim}$	HP operation limits (kW)
$\boldsymbol{S_{ice,c}}$	Centralized ICE size
$S_{ice,lim,c}$	Centralized ICE size limits (kW)
S_{pvp}	Size of the PV panels equipment
$\boldsymbol{S_{stp}}$	Size of the solar equipment
$\boldsymbol{S_{stp,c}}$	Size of the central solar field
$\boldsymbol{S_{ts}}$	Thermal storage size (kWh)
$\boldsymbol{S_{ts,c}}$	Central thermal storage size (kWh)
u, v	Generic unit
v_p	Velocity of the medium inside the pipeline (m/s)
$\boldsymbol{V_{ts}}$	Thermal storage volume (m^3)
wgt	Time interval weight
$\boldsymbol{X_{abs}}$	ABS existence (binary)
$\boldsymbol{X_{boi,c}}$	Central BOI existence (binary)
$\boldsymbol{X_{cp}}$	Existence of the cooling pipeline (binary)
$\boldsymbol{X_{hp}}$	HP existence (binary)

X_{ice}	ICE existence (binary)
$X_{ice,c}$	Centralized ICE existence (binary)
X_{mgt}	MGT existence (binary)
X_{net}	Existence of a network pipeline (binary)
$X_{net,c}$	Existence of the central DHN (binary)
X_{tp}	Existence of the thermal pipeline (binary)

Acronims

ABS	Absorption chiller
BOI	Boiler
CC	Compression chiller
CHP	Combined cooling heat and power
COP	Coefficient of performance
CS	Cooling storage
DCN	District cooling network
DG	Distributed generation
DHCN	District heating and cooling network
DHN	District heating network
HP	Heat pump
ICE	Internal combustion engine
MGT	Micro gas turbine
MILP	Mixed integer linear programming
PV panels	Photovoltaic panels
ST field	Solar thermal field
ST panels	Solar thermal panels
TS	Thermal storage

References

1. Baños, R.; Manzano-Agugliaro, F.; Montoya, F.G.; Gil, C.; Alcayde, A.; G'omez, J. Optimization methods applied to renewable and sustainable energy: A review. *Renew. Sustain. Energy Rev.* **2011**, *15*, 1753–1766. [CrossRef]
2. Henning, D. Energy System Optimization Applied to Local Swedish Utilities. Ph.D. Thesis, Linkopings University, Linköping, Sweden, 1992.
3. Henning, D. MODEST—An energy system optimisation model applicable to local utilities and countries. *Energy* **1997**, *22*, 1135–1150. [CrossRef]
4. Curti, V.; von Spakovsky, M.R.; Favrat, D. An environomic approach for the modeling and optimization of a district heating network based on centralized and decentralized heat pumps, cogeneration and/or gas furnace. Part I: Methodology. *Int. J. Therm. Sci.* **2000**, *39*, 721–730. [CrossRef]
5. Yokoyama, R.; Hasegawa, Y.; Ito, K. A MILP decomposition approach to large scale optimization in structural design of energy supply systems. *Energy Convers. Manag.* **2002**, *43*, 771–790. [CrossRef]
6. Karlsson, M. The MIND method: A decision support for optimization of industrial energy systems principles and case studies. *Appl. Energy* **2011**, *88*, 577–589. [CrossRef]
7. Ortiga, J.; Bruno, J.C.; Coronas, A.; Grossman, I.E. Review of optimization models for the design of polygeneration systems in district heating and cooling networks. In *ESCAPE17*; Elsevier: Amsterdam, The Netherlands, 2007; pp. 1–6.
8. Pohekar, S.D.; Ramachandran, M. Application of multi-criteria decision making to sustainable energy planning—A review. *Renew. Sustain. Energy Rev.* **2004**, *8*, 365–381. [CrossRef]
9. Bazmi, A.A.; Zahedi, G. Sustainable energy systems: Role of optimization modeling techniques in power generation and supply—A review. *Renew. Sustain. Energy Rev.* **2011**, *15*, 3480–3500. [CrossRef]
10. Liew, P.Y.; Theo, W.L.; Alwi, S.R.W.; Lim, J.S.; Manan, Z.A.; Klemeš, J.J.; Varbanov, P.S. Total Site Heat Integration planning and design for industrial, urban and renewable systems. *Renew. Sustain. Energy Rev.* **2017**, *68*, 964–985. [CrossRef]

11. Munoz, J.R. Optimization Strategies for the Synthesis/Design of Highly Coupled, Highly Dynamic Energy Systems. Ph.D. Thesis, Virginia Polytechnic Institute and State University, Blacksburg, VA, USA, 2000.
12. Li, H.; Nalim, R.; Haldi, P.A. Thermal-economic optimization of a distributed multi- generation energy system—A case study of Beijing. *Appl. Therm. Eng.* **2006**, *26*, 709–719. [CrossRef]
13. Kavvadias, K.C.; Maroulis, Z.B. Multi-objective optimization of a trigeneration plant. *Energy Policy* **2010**, *38*, 945–954. [CrossRef]
14. Chinese, D.; Meneghetti, A. Optimisation models for decision support in the development of biomass-based industrial district-heating networks in Italy. *Appl. Energy* **2005**, *82*, 228–254. [CrossRef]
15. Söderman, J.; Pettersson, F. Structural and operational optimisation of distributed energy systems. *Appl. Therm. Eng.* **2006**, *26*, 1400–1408. [CrossRef]
16. Pavicevic, M.; Novosel, T.; Puksec, T.; Duic, N. Hourly optimization and sizing of district heating systems considering building refurbishment—Case study for the city of Zagreb. *Energy* **2017**, *137*, 1264–1276. [CrossRef]
17. Pérez-Mora, N.; Lazzeroni, P.; Martínez-Moll, V.; Repetto, M. Optimal management of a complex DHC plant. *Energy Convers. Manag.* **2017**, *145*, 386–397. [CrossRef]
18. Ameri, M.; Besharati, Z. Optimal design and operation of district heating and cooling networkswith CCHP systems in a residential complex. *Energy Build.* **2016**, *110*, 135–148. [CrossRef]
19. Ren, H.; Zhou, W.; Nakagami, K.; Gao, W.; Wu, Q. Multi-objective optimization for the operation of distributed energy systems considering economic and environmental aspects. *Appl. Energy* **2010**, *87*, 3642–3651. [CrossRef]
20. Carvalho, M. Thermoeconomic and Environmenal Analyses for the Synthesis of Poly- Generation Systems in the Residential-Commercial Sector. Ph.D. Thesis, University of Zaragoza, Zaragoza, Spain, 2011.
21. Ito, K.; Yokoyama, R. A revised decomposition method for MILP problems and its application to operational planning of thermal storage systems. *J. Energy Resour. Technol.* **1996**, *118*, 227–235.
22. Ito, K.; Akagi, S. An optimal planning method for a marine heat and power generation plant by considering its operational problem. *Int. J. Energy Res.* **1986**, *10*, 75–85. [CrossRef]
23. Ito, K.; Yokoyama, R. Optimal operational planning of cogeneration system with thermal storage by the decomposition method. *J. Energy Resour. Technol.* **1995**, *117*, 337–343.
24. Silva, V.V.; Fleming, P.J.; Sugimoto, J.; Yokoyama, R. Multiobjective optimization using variable complexity modelling for control system design. *Appl. Soft Comput.* **2008**, *8*, 392–401. [CrossRef]
25. Lazzarin, R.; Noro, M. Local or district heating by natural gas: Which is better from energetic, environmental and economic point of views? *Appl. Therm. Eng.* **2006**, *26*, 244–250. [CrossRef]
26. Dobersek, D.; Goricanec, D. Optimisation of tree path pipe network with non- linear optimisation method. *Appl. Therm. Eng.* **2009**, *29*, 1584–1591. [CrossRef]
27. Verda, V.; Baccino, G.; Sciacovelli, A.; Russo, S.L. Impact of district heating and groundwater heat pump systems on the primary energy needs in urban areas. *Appl. Therm. Eng.* **2012**, *40*, 18–26. [CrossRef]
28. Rezaie, B.; Rosen, M.A. District heating and cooling: Review of technology and potential enhancements. *Appl. Energy* **2011**, *93*, 2–10. [CrossRef]
29. Tveit, T.; Savola, T.; Gebremedhin, A.; Fogelholm, C. Multi-period MINLP model for optimising operation and structural changes to CHP plants in district heating networks with long-term thermal storage. *Energy Convers. Manag.* **2009**, *50*, 639–647. [CrossRef]
30. Badyda, K.; Bujalski, W.; Milewski, J.; Warcho, M. Heat accumulator in large district heating systems—Simulation and optimisation. In Proceedings of the ASME Turbo Expo 2010, Glasgow, UK, 14–18 June 2010; pp. 1–6.
31. Domínguez-Muñoz, F.; Cejudo-López, J.M.; Carrillo-Andrés, A.; Gallardo-Salazar, M. Selection of typical demand days for CHP optimization. *Energy Build.* **2011**, *43*, 3036–3043. [CrossRef]
32. Ortiga, J.; Bruno, J.C.; Coronas, A. Selection of typical days for the characterisation of energy demand in cogeneration and trigeneration optimisation models for buildings. *Energy Convers. Manag.* **2011**, *52*, 1934–1942. [CrossRef]
33. International Energy Agency. *Co2 Emissions from Fuel Combustion*; IEA Publications: Paris, France, 2011.
34. Marler, R.T.; Arora, J.S. Survey of multi-objective optimization methods for engineering. *Struct. Multidiscip. Optim.* **2004**, *26*, 369–395. [CrossRef]

35. Italian Parlament. *D.lgs. 79/99 Electricity and Gas Italian Market Liberalization*; Italian Parliament: Roma, Italy, 1999.
36. Italian Parlament. *D.Lgs 70/07 Implementation of the EU Directive 2008/4/Ce*; Italian Parliament: Roma, Italy, 2007.
37. Italian Parlament. *Decree July 5th, 2012: Quinto Conto Energia*; Italian Parliament: Roma, Italy, 2012.